Elastohydrodynamic lubrication in spur and helical gear contacts

Sudeendra Chitta

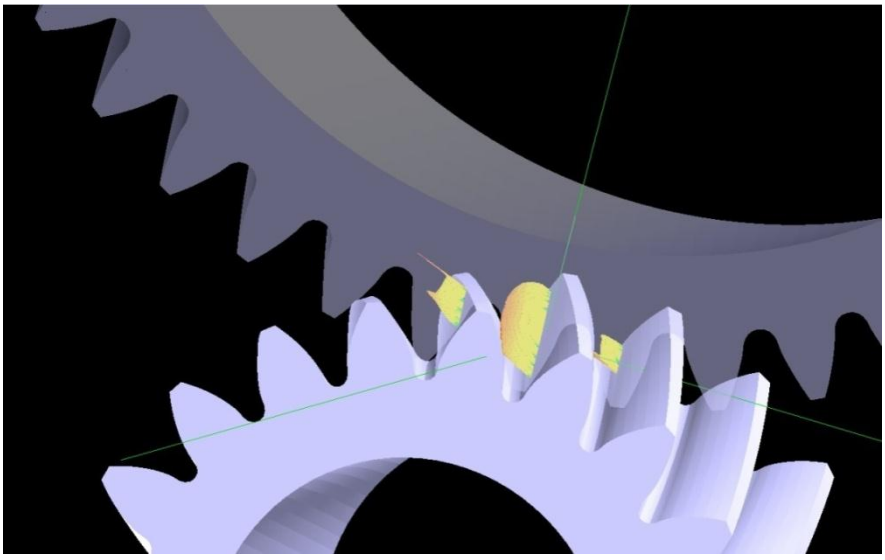

Master of Science Thesis MMK 2012:77 MKN 073
KTH Industrial Engineering and Management
Machine Design
SE-100 44 STOCKHOLM

KTH Industriell teknik och management

Examensarbete MMK 2012:77 MKN 073

Elastohydrodynamisk smörjning i cylindriska och snedskurna kugghjulskontakter

Sudeendra Chitta

Godkänt	Examinator	Handledare
2012-11-29	Ulf Sellgren	Stefan Björklund
	Uppdragsgivare	Kontaktperson
	Scania CV AB	Mats Henriksson

Sammanfattning

Kugghjulen i en växellåda är smorda för att förhindra haveri på grund av lokala korrosionsskador, s.k. pitting, och nötning av kuggytorna. Smörjmedlet verkar även som kylmedel och förhindrar uppkomsten av för höga yttemperaturer, vilket i sin tur kan leda till lokal svetsning, s.k. scuffing**.**

Syftet med detta examensarbete är bygga en realistisk beräkningsmodell för smörjning av raka och sneda kugghjul. De sökta utdataparametrarna var i huvudsak filmtjocklek och lokala yttemperaturer, es.k. flashtemperturer, vilka skulle kunna användas vid identifiering av kuggytor som löper stor risk med avseende på de tidigare nämnda felmoderna. Detta examensarbete genomfördes i samarbete med institutionen för Maskinkonstruktion vid Kungliga Tekniska Högskolan i Stockholm.

Kugghjulssmörjning är ett komplext problem eftersom det kräver kunskap om parametrar som laster, krökningar och hastigheter, vilka är svåra att bestämma över hela kuggytan. Svårigheterna ligger främst i att lasterna är dynamiska till sin natur**,** under rörelsen fördelas dessutom lasten mellan olika kuggpar. Beräkning av hastigheter och krökningar i ett profilmodifierat område i toppen av kuggflanken som kallas ”tip-relief” kan inte heller göras på ett enkelt sätt. Dessa problem förenklades till stor del med hjälp av programmet Helical 3D. Med dess kraftfulla kontaktanalysalgoritm kunde värden för filmtjocklek och flashtemperaturer bestämmas i nästan varje område där kontakt inträffade mellan kuggarna.

Resultatet av modellen visade en minskning av filmtjockleken i ”tip-relief”-området av kugghjulens tandyta, vilket innebär att det fanns en högre risk för förekomsten av pitting och nötning i området. Detta bekräftades senare genom fotografier från experimentella tester vilka visade en pittinglinje i ”tip-relief” regionen på sneda kugghjul. Beräkningsmodellen visade också att förekomsten av pitting kunde kraftigt reduceras om en kvadratisk ”tip-relief**”** användes istället för den nuvarande linjära som används på Scania. En annan viktig slutsats var att de termiska effekterna gav till en betydande minskning av filmtjockleken. Beräkningsmodellen visade dessutom högre flashtemperaturer nära toppen av tandytan och på fotografier, tagna i området från gjorda experiment kunde man se scuffing-märken.

KTH Industrial Engineering and Management

Master of Science Thesis MMK 2012:77 MKN 073

Elastohydrodynamic lubrication in spur and helical gear contacts

Sudeendra Chitta

Approved	Examiner	Supervisor
2012-11-29	Ulf Sellgren	Stefan Björklund
	Commissioner	Contact person
	Scania CV AB	Mats Henriksson

Abstract

The gears in a transmission are lubricated to prevent their premature failure as a result of pitting and wear on the tooth surfaces. Furthermore, the lubricant also limits the rise in surface temperature of the gears, which could otherwise lead to failure as a result of scuffing.

The purpose of this thesis was to construct a fairly realistic theoretical lubrication model for spur and helical gears, the primary output parameters of this model being film thickness and flash temperatures, which would help in the identification of areas on the gear tooth surface prone to the aforementioned modes of failure. This thesis was carried out at the Gear Technology group in Scania CV AB in collaboration with the department of machine design at KTH.

Gear lubrication is tricky as it entails the determination of parameters such as loads, curvatures, and velocities; which are different along the entire surface of the gear tooth. Primarily the loads are hard to obtain as they are dynamic in nature; the load is shared between different pairs of teeth during motion. The calculation of velocities and curvatures in an area of the gear surface called the tip relief can also not be done in a straightforward manner. These issues were simplified to a large extent with the assistance of a program called Helical 3D; owing to its powerful contact analysis algorithm, values of the film thickness and flash temperatures could be determined in almost every region where contact occurred between the gear teeth.

The results of the lubrication model showed a reduction in film thickness in the tip relief area of the gear tooth surface; which meant that there were higher chances for the incidence of pitting and wear in this region. This was later confirmed when photographs from experimental tests illustrated a pitting line in the tip relief region of the helical gear. It was also inferred from the model that the occurrence of pitting could be greatly reduced if a quadratic tip relief modification were applied when compared to the existing linear modification used at Scania. Another important conclusion drawn was that thermal effects contributed to a significant decrease in the film thickness. Furthermore, the model showed higher flash temperatures close to the tip of the gear tooth surface, and photographs from experiments conducted showed the presence of scuffing marks there.

FOREWORD

I would like to thank the following individuals for their invaluable guidance and assistance provided during the course of this thesis.

Mats Henriksson, my supervisor at Scania CV AB for having been an excellent guide, always willing to help and offer suggestions. It was a privilege working with him.

Sandeep Vijayakar, for being so patient and answering questions pertaining to Helical 3D.

My colleagues within the Gear Technology group at Scania, Erik Sandqvist (manager), Niklas Melin, Shadi Khatibi, Joel Axelsson, Johan Wållgren, and Anders Stenman; for offering help and advice whenever needed.

Hubert Herbst and Henrik Åström from the engine development division at Scania, for taking part in the discussions and providing valuable information.

Stefan Björklund, academic supervisor for regularly keeping in touch, providing relevant literature and indicating whether I was going in the right direction or not.

To my teachers, Ulf Sellgren, Ulf Olofsson, and Ellen Bergseth for their help and guidance.

My good friend Simon Chamoun for helping me with the Swedish version of the abstract.

Finally, a big thanks to Scania CV AB for having given me this wonderful opportunity.

Sudeendra Chitta

Stockholm October 2012.

NOMENCLATURE

Notations and abbreviations used in this thesis.

Notations

Symbol	*Description*
R	Pitch Circle Radius (m)
ψ	Pressure angle (rad)
Ω	Angular Velocity (rad/s)
α	Pressure-viscosity coefficient (Pa^{-1})
E	Effective Young's Modulus (N/m^2)
η	Viscosity (Pa-s)
W	Contact Load (N)
Φ_n	Normal Pressure Angle (rad)
Φ_t	Transverse Pressure Angle (rad)
μ	Coefficient of friction
w	Contact load per unit length (N/m)
z	Contact width (m)
U	Rolling velocity
λ	Thermal Conductivity of tooth face material (W/mK)
ρ	Density of gear material (Kg/m^3)
c	Specific Heat of tooth face material (J/KgK)
W^1	Contact Load per unit length (lbf/in)
V_s	Sliding Velocity (in/s)
V_r	Rolling Velocity (in/s)
P_H	Hertzian Pressure (N/m^2)
E^1	Equivalent Modulus of Elasticity (N/m^2)
h_m	Minimum Film Thickness (μm)
σ	Composite Surface Roughness (μm)
L_{in}	Input Torque (Nm)
w_{in}	Input speed of pinion (rad/s)
R_A	Addendum radius (m)
Ψ_s	Transverse working pressure angle (rad)
G	Gear Ratio
a	Centre to centre distance (m)

Z	Number of teeth
m	Module
τ	Pressure angle (rad)
β	Helix angle (rad)
ω	Angular Velocity (rad/s)
K_f	Lubricant Thermal conductivity (W/mK)
$d\eta/dt_m$	Viscosity-temperature slope (Pa-s/^oK)

*Note: Subscripts 1 and 2 denote pinion and gear respectively

Abbreviations

ANSOL	Advanced Numerical Solutions
FEM	Finite Element Analysis
AGMA	American Gear Manufacturer's Association

TABLE OF CONTENTS

1 INTRODUCTION

This chapter presents the background, purpose, delimitations and a brief description of the method used in this project.

1.1 Background

The gears in an automotive transmission are lubricated to prevent the premature wear of gear tooth surfaces and reduce the friction. The lubricant also serves to decrease the amount of operating noise in the transmission; and limit the rise of temperature in the gears due to the sliding friction. As a result, a power transmission with high mechanical efficiency is achieved with the individual components, i.e., the gears in this case, having a good reliability and life time. (Van Beek, 2006). Therefore a thorough understanding of gear lubrication is essential in order to be able to predict good lubricant performance and also to estimate the losses due to friction.

Scania CV AB is a leading manufacturer of heavy trucks, buses, and coaches based in Södertälje Sweden. The *Gear Technology* group under the *Transmission Development* division is committed towards developing a better understanding of the role played by the gears in a transmission. Their main responsibilities include gear design and analysis; and conducting fatigue and acoustic tests.
Furthermore, with regards to lubrication, the group mainly relies on experimental testing to estimate the probability of pitting and wear, which are common modes of failure that occur due to improper lubrication on the gear tooth surfaces. The outcome of this thesis would be the development of a fairly realistic theoretical lubrication model that uses a novel finite element approach and this serves as a good add-on to the existing method; as such an approach would yield fairly accurate results and the model would provide a better understanding of the various parameters involved and thereby help in further analysis.

1.2 Purpose

The primary objective of this thesis is to develop a realistic lubrication model; its main output being an important parameter known as the film thickness (explained later in section 2.6) along the profile and face of the gear tooth. Knowledge of the film thickness helps in identifying areas on the gear tooth that are more prone to wear. Also, of particular interest is the value of this film thickness on an area of the gear tooth known as the tip relief.
Other parameters such as the flash temperature, friction co-efficient, and losses in the gear mesh are also determined. The probability of failure due to scuffing can be known from the flash temperature.

1.3 Delimitations

This thesis is delimited in validation and analysis. A thorough comparison with previously determined theoretical/experimental data could not be done, as this data was not available. Moreover, a detailed parameter analysis was not conducted. Most of the implementation was done for only a specific set of gears and lubricant; it would have been interesting to see the influence of different gear sizes, materials, input torques, and lubricants on the output parameters such as the film thickness and flash temperatures.

The lubrication model that was developed is valid only for spur and helical gears, not for other gear types such as bevel, hypoid, and planetary gears.

1.4 Method

The basic approach for this thesis was to initially begin with an elementary model having a number of assumptions, and gradually build on the complexity by reducing these assumptions and adding more features until a fairly complex lubrication model was developed at the end. The Fig. (1) illustrates this:

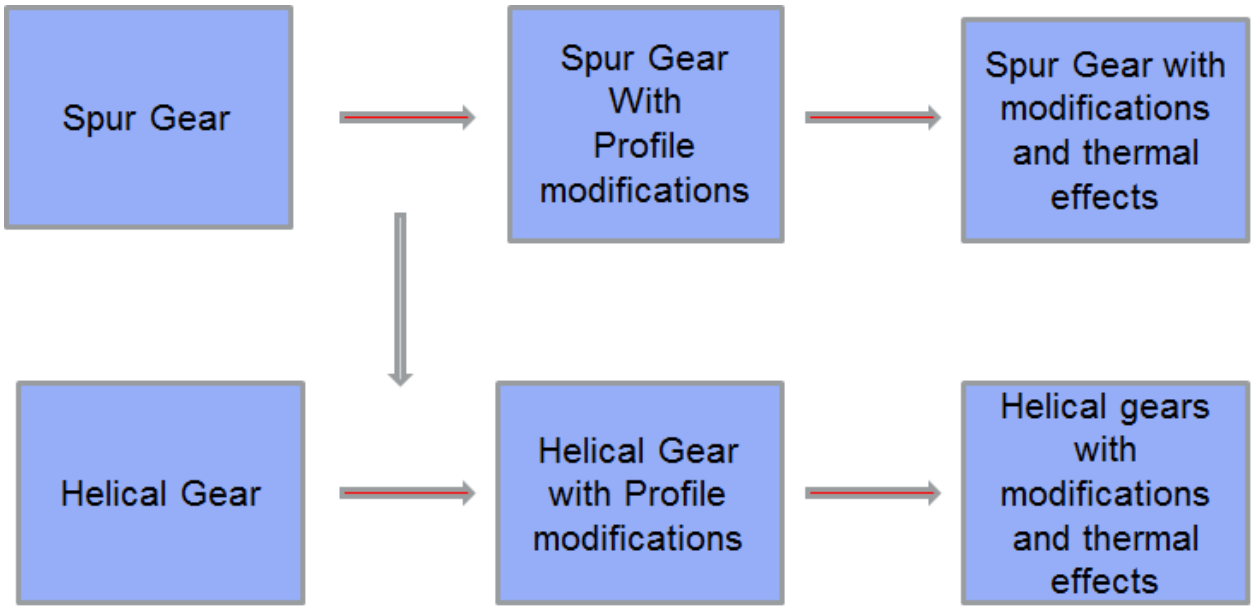

Figure1, Arriving at the realistic model

The lubrication model was first constructed for spur gears, and then profile modifications were applied on the gear tooth. Thermal effects were also brought into the model in order to make it even more realistic. These two features will be explained later.
This was extended to helical gears; until arriving at a realistic model, which is for helical gears with profile modifications and thermal effects.

The two softwares that were used in this thesis were Helical 3D and MATLAB. Helical 3D is a tool capable of performing finite element contact analysis on spur and helical gears. It was developed by ANSOL, ltd.
The main lubrication model was constructed in MATLAB. This required a number of gear geometry parameters; which were obtained as a result of the contact analysis simulations performed in Helical 3D. The final results were obtained from the MATLAB model, and these were the film thickness, friction co-efficient, flash temperatures, and losses.

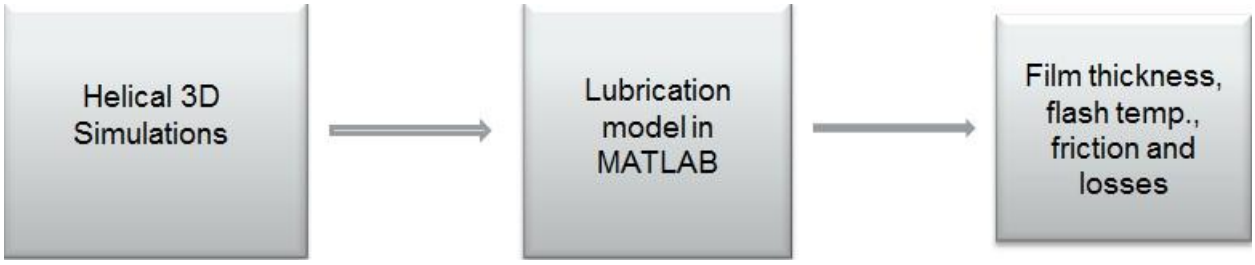

Figure 2, Flowchart illustrating procedure

A detailed description of the method can be found in Chapter 3.

2 FRAME OF REFERENCE

The reference frame is a summary of the existing knowledge and former performed research on the subject. This chapter presents the theoretical reference frame that is necessary for the construction of the lubrication model.

2.1 Gears

Gears are toothed members which transmit power/motion between two shafts by meshing without any slip (Gopinath; Mayuram). The pinion is the name given to the smaller of the two mating gears, the larger one is known as the gear or the wheel (Uicker, 2003). They are classified based on the shape of the tooth pair and the angle between the axes of the two mating gears. The Fig. (3) illustrates basic gear terminology.

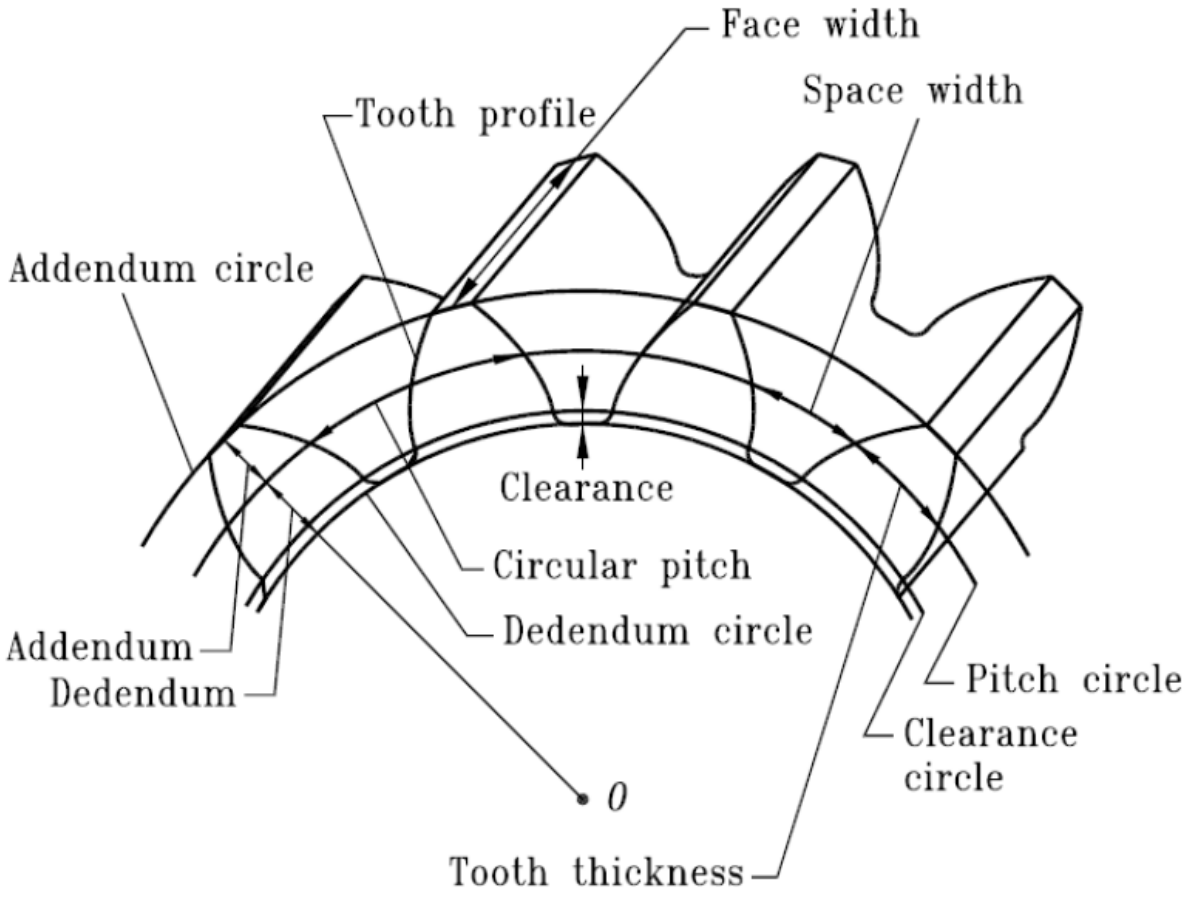

Figure 3, Basic Gear Nomenclature (Litvin, 2004)

As mentioned earlier in section 1.4, two types of gears are being dealt with in this case: spur gears and helical gears. The main difference is that in spur gears, the teeth are parallel to the axis whereas the teeth are inclined to the axis in helical gears. The Fig. (4) shows these two types of gears.

Figure 4, Spur gears (left) and helical gears (right)

Spur gears are simple in construction and are easier to manufacture. Helical gear operation is smoother and quieter and they are also capable of handling very high speeds and loads due to which they find application in automotive gearboxes.

2.2 Involute Roll Angle

The shape of the gear tooth is an involute curve; and any point along this involute profile from the root till the tip of the gear tooth can be represented by means of the involute roll angle.

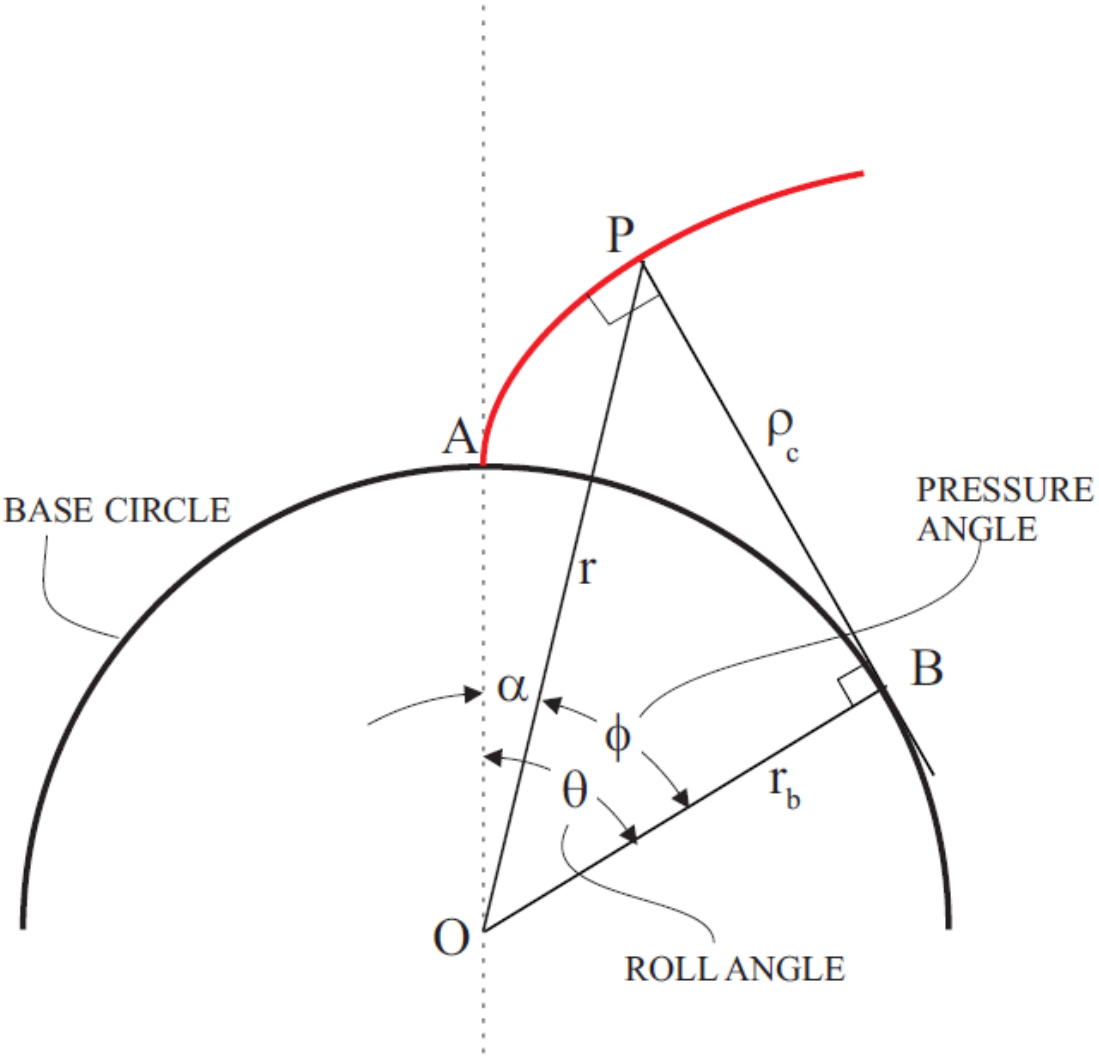

Figure 5, Involute Roll angle (Helical 3D Manual, 2005)

A roll angle of 0^o would correspond to the root and an angle of, say, 35^o would mean the tip.

2.3 Profile modifications

In order to make the lubrication model more realistic, profile modifications were applied on the gear tooth. This was done by making use of the Helical 3D software. Generally, three kinds of profile modifications are applied.

- Profile Crowning
- Lead Crowning
- Tip Relief

In this analysis, all three modifications were applied on the helical gear whereas only a tip relief modification was applied on the spur gear. Profile crowning is a curvature along the profile and lead crowning is the curvature of the gear tooth along the face. Tip relief is a thinning of the tooth (material removal) close to the tip (Dudley, 1984). It is done in order to facilitate smoother engagement of the gears. It is basically a function of the following three parameters; mode, roll angle, and magnitude.

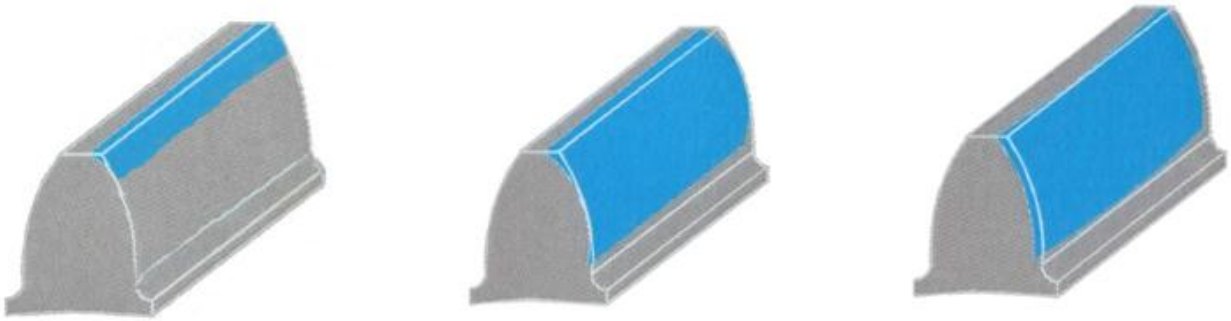

Figure 6 (L-R), Tip Relief, Profile crowning, Lead crowning (Courtesy Scania)

The mode denotes linear or quadratic; roll angle is the point on the profile where the tip relief actually starts. The magnitude is the amount of material that is removed. The Figs. (7) and (8) illustrate both linear and quadratic tip relief modifications.

The straight line signifies the following: from the root till the point where the tip relief starts, the profile is a perfect involute. The inclined line in the case of linear tip relief and the parabolic curve in the case of the quadratic tip relief denote the manner in which there is a deviation from the perfect involute profile of the gear tooth.

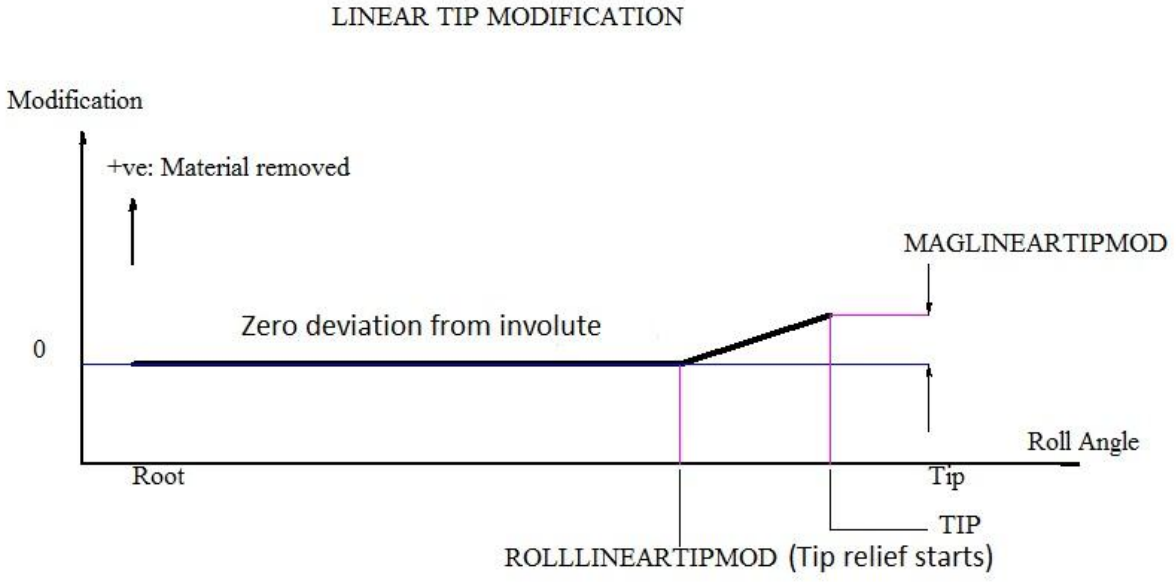

Figure 7, Linear Tip relief (Helical 3D manual, 2005)

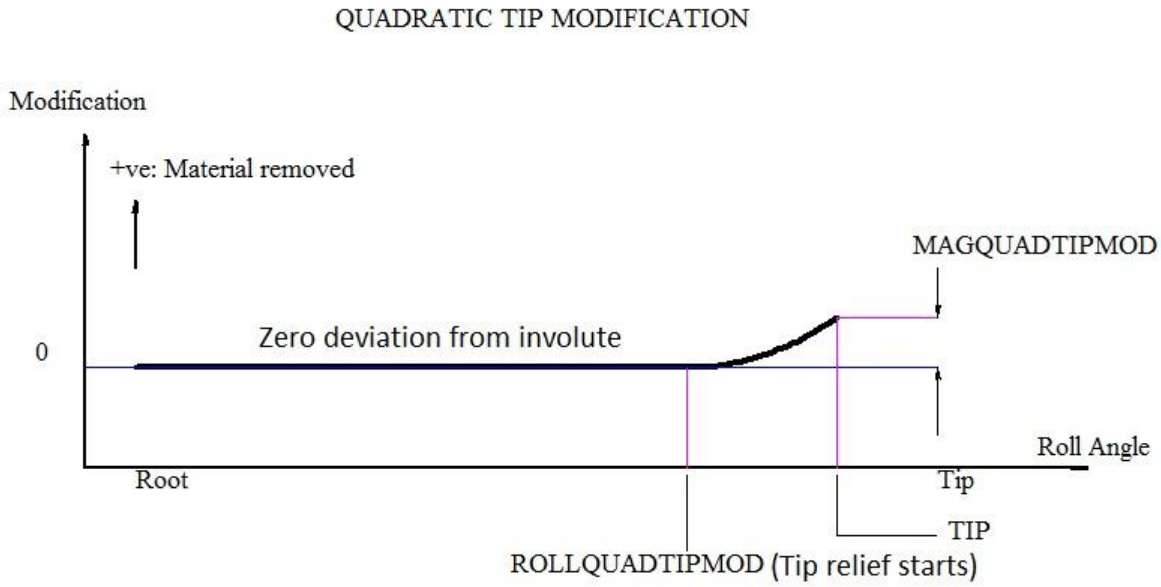

Figure 8, Quadratic Tip relief (Helical 3D manual, 2005)

2.4 Elastohydrodynamic Lubrication

Elasto-hydrodynamic lubrication is the mechanism that describes the separation by a lubricant film (shown in Fig. (9)) between two elastic machine elements in either point or line contact, that are loaded against each other and are in relative motion (Gohar, 2001). Such conditions arise in gears, cams, and rolling element bearings and the type of contact is referred to as non-conformal (Van Beek, 2006). While the contact is typically a line contact in the case of spur gears, the contact varies from a point to that of a line along the engagement of the mating teeth in a helical gear.

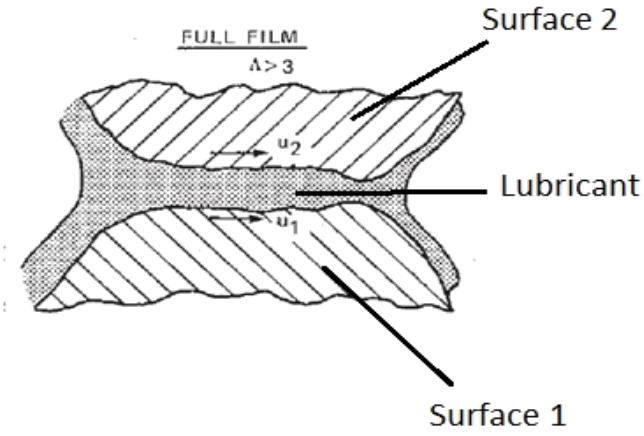

Figure 9, Lubricant film formation between two surfaces (Cheng, 1983)

The primary aim in the analysis is to determine the thickness of this lubricant film, also known as the film thickness. In general, the thickness is in the order of microns, and is comparable to the height of the surface asperities.

Some of the assumptions employed in hydrodynamic theory in the analysis of journal bearings are not valid in the elastohydrodynamic case (Dowson, 1966). The contact loads are in general much higher in comparison with hydrodynamic lubrication. Therefore, the pressure build up in the lubricating film is so high that it significantly affects its viscosity (Dowson, 1966). Furthermore, the contiguous surfaces are elastically distorted as a result of the high pressure rise and this drastically changes the geometry of the lubricating film (Dowson, 1966).
The aforementioned two effects, i.e. pressure-viscosity dependence of the lubricant and the elastic deformations of the bounding surfaces form the basis of the elastohydrodynamic theories. There are also other effects such as thermal and starvation effects; an attempt has been made in this thesis to include thermal effects; i.e. the variation of lubricant viscosity with temperature and heating effects due to the shearing action involved.
Dowson and Higginson (1966) presented a solution to the elastohydrodynamic problem, which is widely accepted even today. A major portion of this thesis has strong foundations in the work of Dowson and Higginson.

2.5 Failure due to improper lubrication

Three modes of failure in gears due to improper lubrication are:

- Pitting

When a particle of material breaks away from the sliding surface after a large number of contact cycles, then pitting (Fig. (10)) or surface fatigue is said to occur (Van Beek, 2006).

Figure 10, Pitting on a gear surface (Courtesy Scania)

- Scuffing

Damage on the surface due to the welding of microasperities between the bounding surfaces (Tobe, 2000).

- Wear

It is the phenomena of material removal from the mating surfaces under thin film operating conditions. A small amount of it is actually necessary for bettering the conformity of the surfaces. (NASA)

2.6 Minimum film thickness

This section explains the basic equations for determining the film thickness between two involute spur gears in contact.
The contact between involute spur gear teeth at any point along the meshing cycle (or line of action) can be represented by two equivalent cylinders (darker circles) as shown in the Fig. (11).

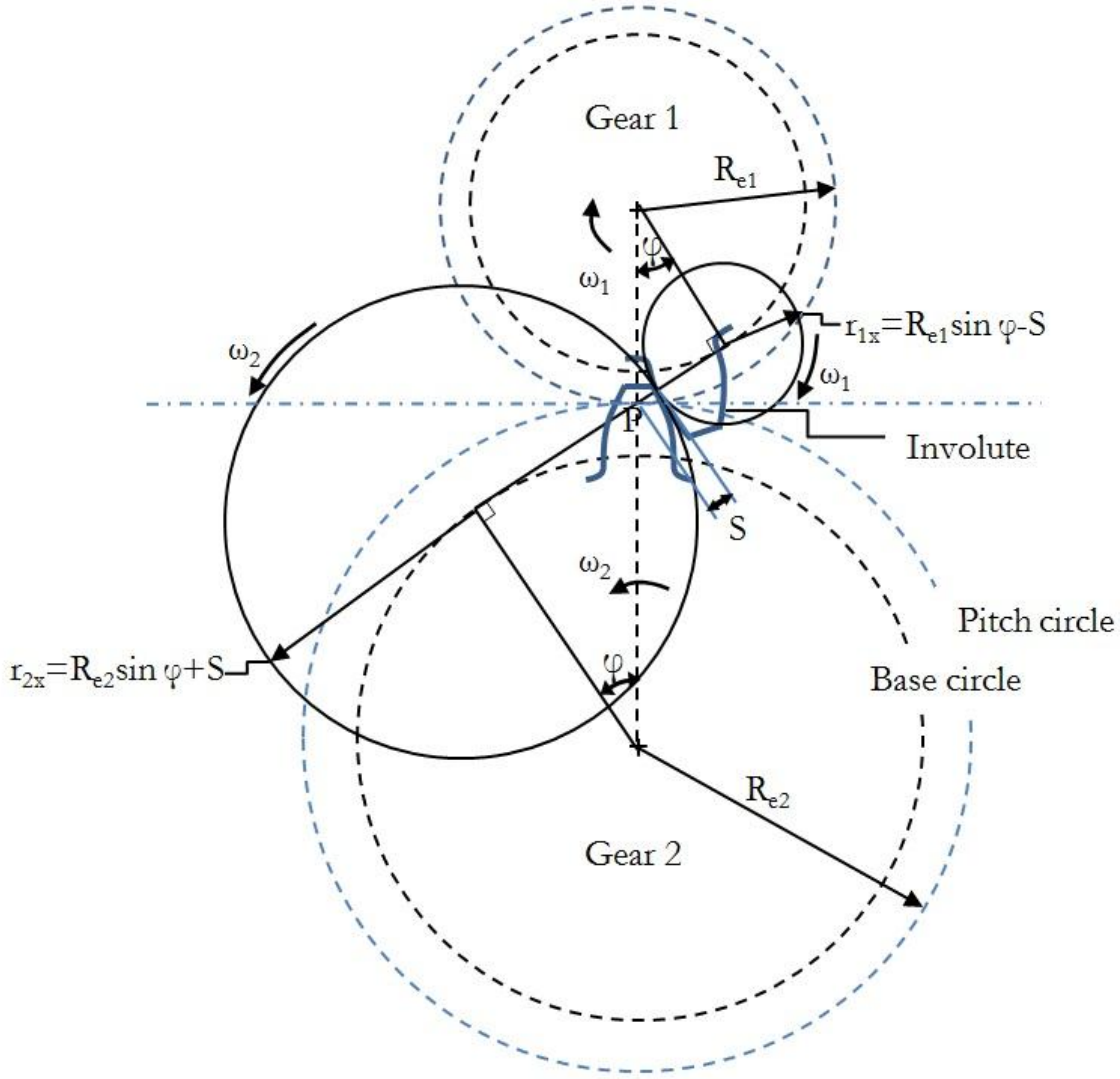

Figure 11, Contact between two gears analogised as two cylinders in contact (Courtesy Ellen)

From the Fig. (11) it can be readily seen that the radii of the two cylinders vary at different points along the line of action (as the distance s from the pitch point changes), and so do the rolling velocities, represented by U_1 and U_2. Pure rolling occurs at the pitch point, and a combination of rolling and sliding takes place at other points (Uicker, 2003). The tooth load acts

in the direction of the common tangent to the two base circles, which completes the approximate analogy (Dowson, 1966).
This approach was developed by (Merritt, 1942) and thereby adapted by Dowson et al. in their film thickness calculations. In the Fig. (11) the lubricant forms a thin film in between the two cylinders in contact. A more simplified approach shows only one equivalent cylinder near a plane with the lubricant in between.

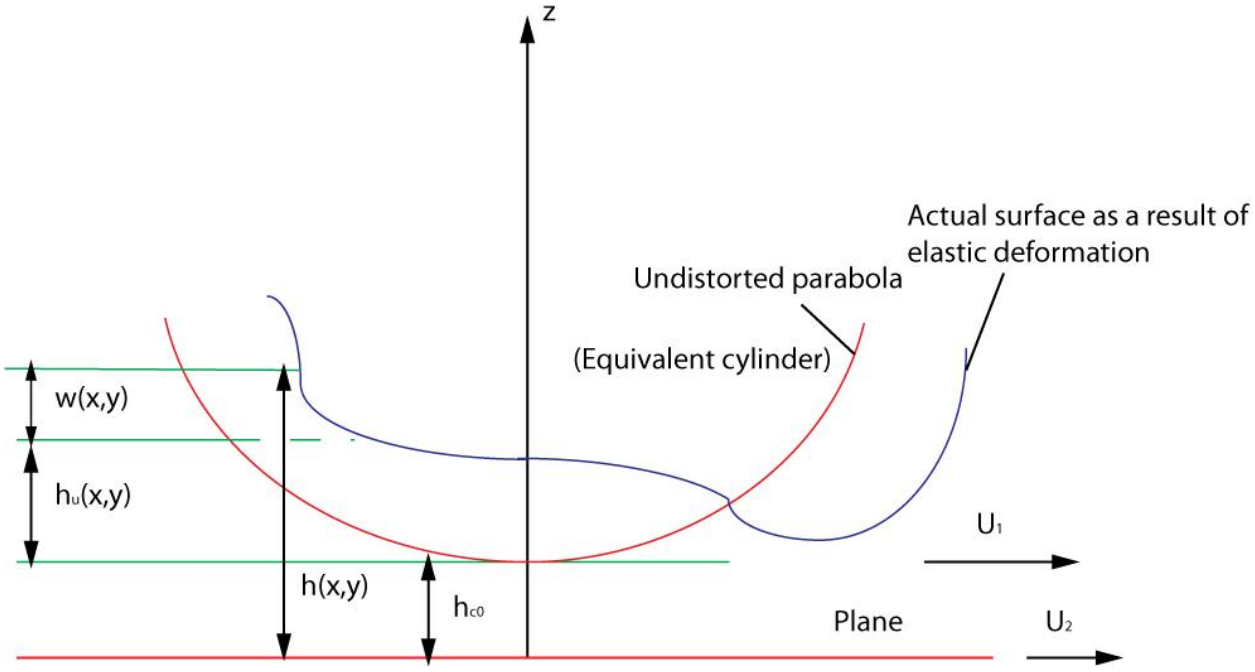

Figure 12, equivalent cylinder and plane

The Fig. (12) shows the actual surface (in blue) that has been distorted as a result of the elastic deformations. The film thickness is h(x,y) and is calculated using the equations derived by Dowson and Higginson.

Dowson and Higginson were actually able to derive an algorithm for computing the distribution of the film thickness along the length of the contact. In the case of gears, this would be at one point along the line of action. If the complete solution were applied, then multiple distributions of the film thickness would have to be derived at every point along the meshing cycle or line of action. This would be too cumbersome and beyond the scope of this thesis. It was therefore decided, that only one value, known as the minimum film thickness **(min(h(x,y))** would be determined at every point along the meshing cycle, so this would lead to a *distribution of the minimum film thickness* along the profile and face of the gear tooth.
The radius of the equivalent cylinder shown in Fig. (12) is known as the relative radius of curvature and is given by the equation:

$$R_R = \frac{(R_1 \sin\psi + s)(R_2 \sin\psi - s)}{(R_1 + R_2)\sin\psi} \qquad (1)$$

where

R_1 and R_2 are the pitch circle radii of pinion and gear respectively in m
ψ is the pressure angle

The speed is the resultant of the rolling and sliding speeds. The combined rolling entrainment velocity of the gear and pinion is given by:

$$U_{combined}=\frac{(R_1 sin\psi+s)\Omega_1+(R_2 sin\psi-s)\Omega_2}{2} \quad (2)$$

Ω_1 and Ω_2 are the angular velocities of pinion and gear

The resultant speed, which is the vector sum of the combined rolling entrainment velocity and the sliding speed is then calculated as:

$$U_{resultant}=\sqrt{U_{combined}^2+(U_1-U_2)^2} \quad (3)$$

where

$$U_1=(R_1 sin\psi+s)\Omega_1 \quad (4)$$

$$U_2=(R_2 sin\psi+s)\Omega_2 \quad (5)$$

The equation for the film thickness h, calculated at every point along the width of the contact is given by (Dowson, 1966):

$$h_{min}=\frac{3.63G^{0.49}U^{0.68}}{W^{0.073}} *R_R \quad (6)$$

where

R_R is the Equivalent Radius of Curvature
G is the materials parameter, defined as $\alpha*E$
U is the speed parameter, defined as $\frac{\eta u}{E*RR}$
W is the load parameter (elliptical conjunctions), defined as $\frac{W}{E*(RR^2)}$
For rectangular conjunctions, W is $\frac{W}{E*(RR*l)}$

α is the pressure-viscosity co-efficient in Pa^{-1}
E is the equivalent modulus of elasticity in N/m^2
η is the viscosity of the lubricant in Pa-s
l is the length of the contact in m
W is the contact load per unit length in N/m

2.7 Flash Temperatures

As the gear teeth come into mesh, the temperature of the metal surfaces as well as the lubricant increases as a result of the sliding action (Tobe, 2000). The lubricant is subjected to shear heating, also referred to as a thermal effect which is explained later in detail in this section. Flash temperature is defined as the instantaneous rise in surface temperature in the zone of contact. The formula for determining the flash temperature was derived by Blok et al. for a sliding hertzian contact; which is the nature of contact in this case.
For a helical gear,

$$T_f = \frac{1.11}{\sqrt{\sin\phi_n \csc\phi_t}} \frac{\mu}{b} \frac{w}{\sqrt{z}} \left|\sqrt{U_1} - \sqrt{U_2}\right| \quad (7)$$

Where b is a thermal contact co-efficient for the tooth face material defined as:

$$b = \sqrt{\lambda \rho c}$$

where

λ is the thermal conductivity of the tooth face material in W/mK
ρ is the density of the gear material in Kg/m^3
c is the specific heat of tooth face material in J/KgK
μ is the co-efficient of friction
w is the contact load per unit length in N/m
z is the contact width in m

Since the flash temperature depends on a number of parameters, it varies along the profile and face of the gear tooth, and in general can rise to several hundreds of degrees (Van Beek, 2006).
Flash temperature is an important criterion for establishing the probability of failure due to scuffing. It is very difficult to determine the flash temperature experimentally (Scania) and therefore heavy reliance is laid upon theoretical calculations.
The flash temperature, as defined earlier, is an 'increase' in the surface temperature when contact between gear teeth occurs.

2.8 Friction Co-efficient

Friction can be defined as the resistance to motion between two surfaces in relative sliding and rolling under dry and/or lubricated conditions (Hai, 2005). Owing to the presence of a lubricant, the friction is due to the relative sliding between gear teeth and also occurs as a result of the viscous shearing of the fluid. Therefore, the friction in gears can be considered as a hybrid of dry and fluid friction (Hai, 2005).
Knowledge of the friction co-efficient helps in determining contact fatigue life, calculation of losses and an understanding of noise and vibration (Hai, 2005).
A number of widely used empirical formulae for the friction co-efficient exist (Hai, 2005).
In this analysis the Benedict-Kelly model for determining the value of μ. This is because the model was developed specifically for gear lubrication; gear geometry parameters such as radii of curvature, velocities, and contact load per unit length are present in the formula. Moreover, the fluid friction part is also taken into account due to the existence of the viscosity term. The AGMA also made a mention of this model to determine the variable value of μ in one of their published papers.

$$\mu = 0.0127 \log_{10}\left[\frac{3.17(10)^8 W^1}{\eta V_s V_r^2}\right] \quad (8)$$

where

W^1 is the contact load per unit length in lbf/in
V_s is the sliding velocity in in/s
V_r is the rolling velocity in in/s

η is the viscosity of the lubricant in Pa-s
The value of the friction co-efficient varies along the profile and face of the gear tooth and hence is determined at various points of contact.

2.9 Thermal Effects

The lubricant shears due to the sliding motion and this increases its temperature, a phenomenon known as viscous heating. Owing to this, the viscosity of the lubricant decreases which in turn affects the thickness of the film. If this important effect is not taken into consideration, then the film thickness values would be much higher. These thermal effects are included in the lubrication model by use of a thermal correction factor, C_t, (Hamrock, 1991).

$$C_t = \frac{1\text{-}13.2\left(\frac{p_H}{E'}\right)(L)^{0.42}}{1+0.213\left(1+2.23A_c^{0.83}\right)L^{0.64}} \tag{9}$$

where

P_H is the max. value of the hertzian pressure in N/m^2
L relates the viscosity to the rise in temperature and is defined as:

$$L = -\left(\frac{d\eta}{dt_m}\right)\frac{U_{resultant}^{\ 2}}{K_f} \tag{10}$$

The slope value $\frac{d\eta}{dt_m}$ was determined from the viscosity-temperature curve for mineral oil given in (Hamrock, 1991).

And A_c is defined as the slide-roll ratio, given by:

$$A_c = 2\frac{(U_2 - U_1)}{(U_1 + U_2)} \tag{11}$$

The value of A_c is the highest at the tips of the gear teeth and zero at the pitch point. Note that (11) is still valid if the value of A_c is zero.

2.10 Roughness Parameter

The lubrication model for this thesis was developed by assuming that the surfaces of the gear pair were smooth, however, this is not the actual case. Implementing a surface roughness model would have been beyond the scope, therefore, a comparison was made between the values of the film thickness and the surface roughness in order to determine whether the lubrication was good or not; this was done with the use of a roughness parameter denoted by Λ (Gohar, 2001).

$$\Lambda = \frac{h_m}{\sigma_t} \tag{12}$$

$$\sigma_t = \sqrt{{\sigma_1}^2 + {\sigma_2}^2} \tag{13}$$

Based on the value of the roughness parameter, the type of lubrication regime can be determined from the Table (1).

Table 1, Lubrication Regimes relating to roughness parameter

Roughness Parameter Λ	**Lubrication Regime**
Λ>3	Full film
1< Λ<3	Mixed
Λ<1	Boundary

The desirable regimes are full film and mixed, in general, gears operate in the mixed lubrication regime (Seireg, 1998). Boundary lubrication is undesirable, as there is almost no lubricant film existing due to which the contact is almost like a dry contact. (Almqvist, 2004).

2.11 Losses and Efficiency

The total losses occurring in a transmission are given by the expression (Hai, 2005):

$$L_{total} = L_t + L_w + L_b \tag{14}$$

The first term on the right hand side of (14), L_t represents the losses that take place as a result of the friction between the gear teeth. L_w are known as windage or churning losses and are a result of the gear blanks revolving in an oil sump which is used for lubricating the gears. L_b are the losses that occur due to bearing friction. In this lubrication model however, only L_t is determined for a helical gear pair.
The instantaneous efficiency of the gear pair is computed as (Hai, 2005):

$$\eta_{eff.} = 1 - \frac{|F_r + F_f|}{L_{in}\omega_{in}}(U_1 - U_2) \tag{15}$$

where

L_{in} is the input torque in Nm
w_{in} is the input speed of the pinion in rad/s

Therefore it can be seen that the tooth losses are a summation of the rolling and sliding frictional forces. Here, only the sliding component is taken into consideration whereas the rolling component is neglected. The sliding frictional force (in Newtons) is given by:

$$F_f = \mu \times W \tag{16}$$

3 IMPLEMENTATION

This chapter explains in detail the working procedure adopted for this thesis. Extraction of the relevant gear parameters by performing simulations in Helical 3D, and a brief description of the construction of the lubrication model in MATLAB to obtain the final outputs are discussed here.

3.1 Helical 3D Simulations

Helical 3D is a finite element software package capable of performing contact analysis on spur and helical gears.
The Fig. (14) is a screenshot from the Helical 3D program. Shown in the figure are pinion and gear, with the input gear as the pinion. The type of gear is a spur gear; note that the procedure for performing simulations on a helical gear is the same.

In order to determine the gear parameters shown in Table (2) along various points on the gear surface, simulations were performed for one mesh cycle (beginning to end of engagement of gear teeth). The total simulation time was 1.1 seconds and this was done along 11 time steps, more values would be obtained if the number of time steps were increased.
The simulation does not take into account the actual rotational speed of the pinion, but a dummy value of the speed which was calculated in the following manner:

$$N = \frac{60}{(Z \times n_{timesteps} \times \delta t_{eachstep})} \tag{17}$$

In the case of spur gears, the value of N was 3.75 r.p.m., scaled accordingly in the MATLAB model later on to 1500 r.p.m.

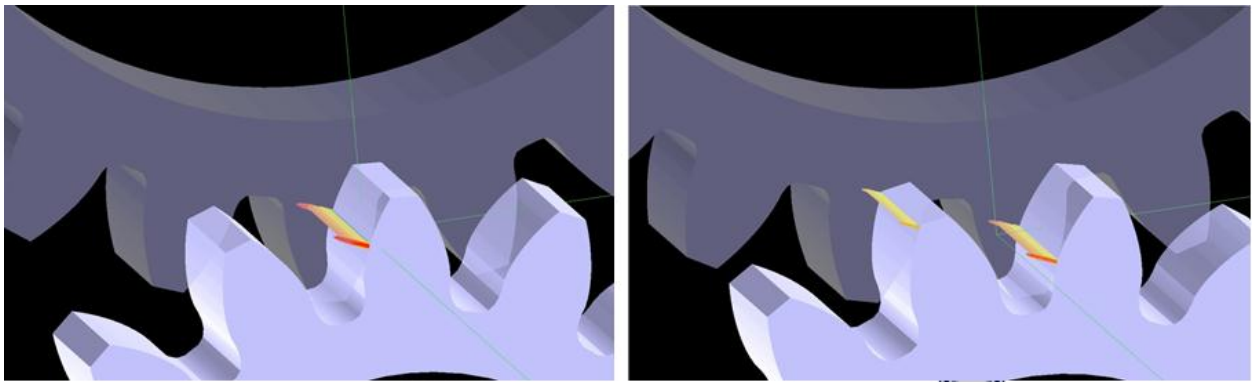

Figure 13, Simulations in Helical 3D (Spur Gear)

A contact grid is formed in the contact zone as shown in the Fig. (14). The grid consists of a number of grid cells of unequal shape and size. There are basically two types of models in action here: A finite element model for large deformations away from the contact zone and an elastic half-space model for obtaining deformations within the contact zone (Hai, 2005).
The grid is represented along the profile direction by means of the vector j and along the face direction by the vector i. Actual contact occurs in the grid cells specified by the red dots, which are also called the principal contact points.
Depending on how fine a grid is needed, the values for m and n have to be specified in Helical 3D. There are 2m+1 and 2n+1 divisions along the profile and face respectively. A finer grid would yield accurate values of the contact pressures.

Table 2, List of parameters calculated from Helical 3D

Normal load per unit length
Hertzian Pressure
Hertzian Semi Width
Contact Load
Relative Radius of Curvature
Rolling velocity
Sliding velocity
Angular velocity

If the number of divisions were given as 9 and 9 along the profile and face, then the total number of grid cells in the contact zone would be 9*9=81. This of course corresponds to one time step. The grid can be made finer by increasing the number of divisions, this was not done since the simulation times were too high.

The calculated parameters, which are determined for only certain specific grid cells are then exported to MATLAB via an export.dat file, where they can be accessed as three dimensional arrays which is shown in Fig. (15). A list of these parameters is shown in table 2.
The data in Fig. (15) corresponds to grid cell no. 6. Likewise, data is stored for the remaining grid cells. For a single time step, as stated earlier there were 81 grid cells, 15 of which contained relevant information.
To store the data of all the 11 time steps, a 1x11 cell matrix was constructed, with each element containing information of the 15 grid cells.
A similar procedure was followed for the other parameters; and a film thickness function was created with all these parameters as the input variables. The final output of the film thickness was therefore a 1x11 cell.

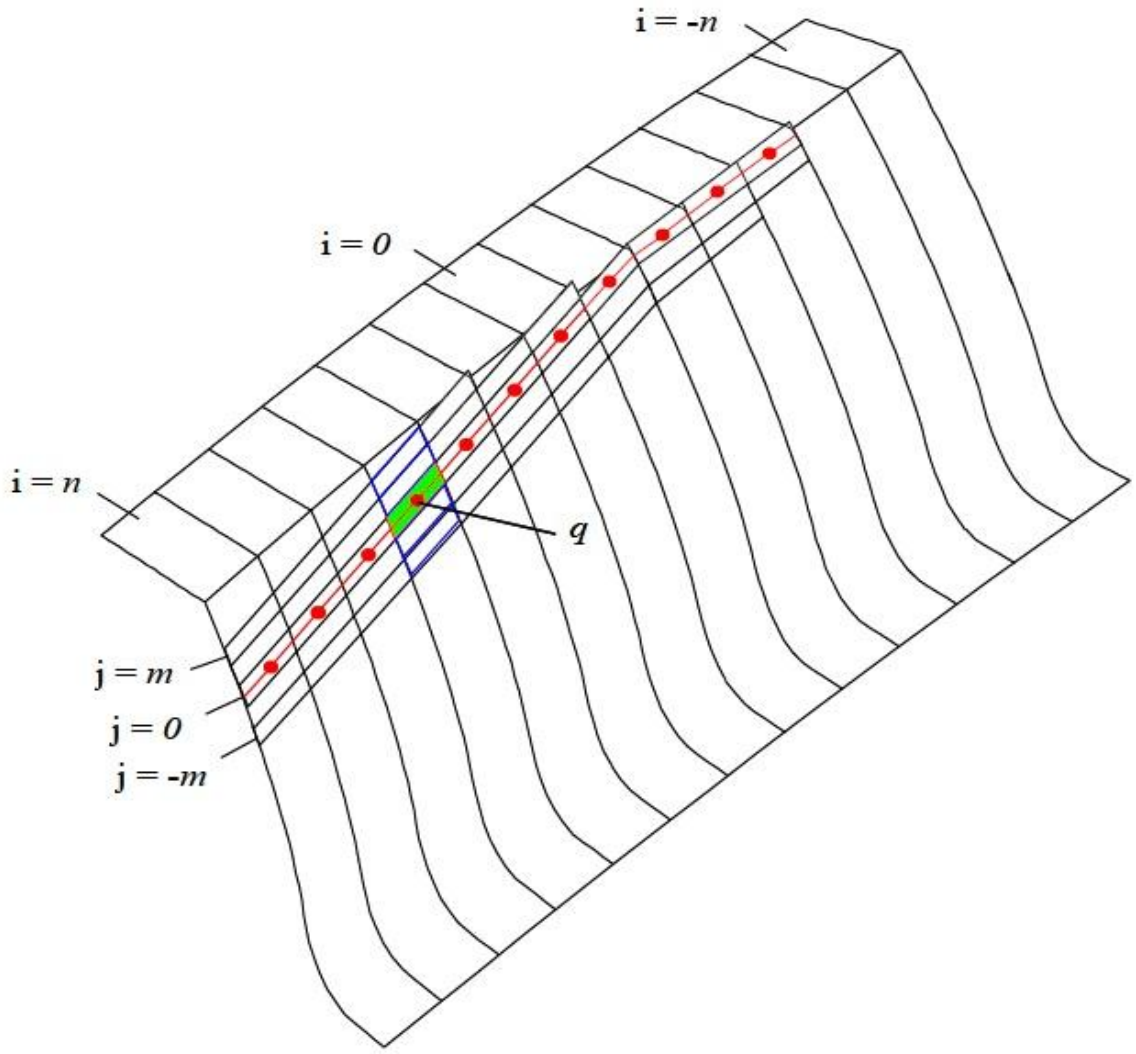

Figure 14, Contact grid formation (Helical 3D manual, 2005)

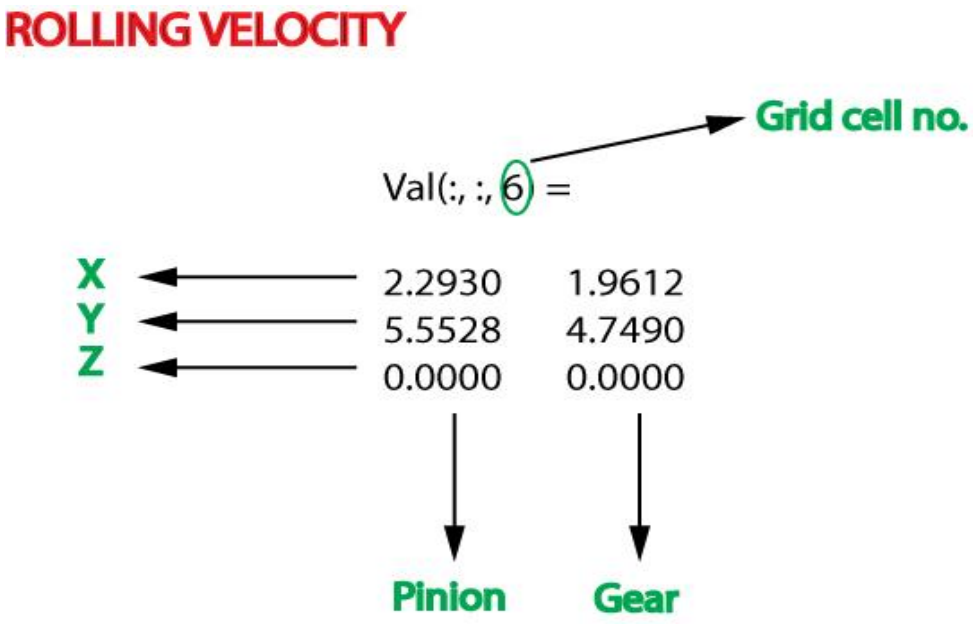

Figure 15, Grid cell data stored as 3-D Array

3.2 Lubrication Model

Functions were created in MATLAB for calculating the film thickness, flash temperature, friction co-efficient, losses, and efficiency from the equations (6), (7), (8), (15), and (16). Special functions were created for both pre and post processing. The preprocessing included reading the data from Helical 3D and squeezing out only the relevant information; postprocessing dealt with plotting the final results.

4 RESULTS

In this chapter, the results are presented and analyzed. Film thickness plots for both spur and helical gears, and flash temperatures, friction co-efficient, and losses for helical gears are shown.

4.1 Simple EHD model results

A literature study was conducted in the initial phase of this thesis. At the end of this study a simple lubrication model was constructed in MATLAB without the use of Helical 3D; in order to get an understanding of the effects of various parameters such as speeds, loads and different lubricants on the film thickness. A description of the construction of this simple model and its results are presented and briefly discussed here.
From (6), it can be observed that the minimum film thickness is dependent on three dimensionless parameters, load, speed, and material. This model was devised based on the following assumptions:

- Sliding velocities are neglected; only rolling occurs along the entire line of action and is a constant.
- The contact load in reality varies in magnitude along the line of action. Also, in general more than one pair of teeth are in contact which implies that the total load is shared between the teeth (referred to as dynamic load sharing). In this scenario, the contact load is assumed to be uniform along the line of action and the contact ratio is taken to be unity.

Gear and lubricant information are provided in appendices (A), (B), and (C).
The basic procedure was to calculate the length of the line of action and then divide this into a number of steps and calculate the value of the film thickness at each step, by assuming values for the load and speed. The detailed steps (Uicker, 2003) are:

Length of path of approach:

$$P_A = \sqrt{{R_{A1}}^2 - {R_1}^2 cos^2\psi} - R_1 sin\psi \tag{18}$$

Substituting parameters from Table (gear data) into eqn. (18),

$$P_A = 11.3 \text{ mm} \tag{19}$$

Length of path of recess:

$$P_R = \sqrt{{R_{A2}}^2 - {R_2}^2 cos^2\psi} - R_2 sin\psi \tag{20}$$

Substituting parameters from Table (gear data) into eqn. (20),

$$P_R = 12 \text{ mm} \tag{21}$$

Where

R_{A1} and R_{A2} are the addendum radii of pinion and gear respectively

Length of path of contact:

$$P_A + P_R = 23.3 \text{ mm} \quad (22)$$

This value of the length was rounded off to 24mm and the entire line of action was divided into 25 steps and computed as a vector s for calculation in MATLAB.
The value of s (radius of curvature eqn.) (in steps of 0.01) now has the range:

$$s = [-12,12] \quad (23)$$

Assumed value of speed:

$$u = 5ms^{-1} \quad (24)$$

Assumed value of load:

$$w = 25000N/m \quad (25)$$

The equivalent radius of curvature was then calculated from (1) and all parameters were substituted in (6) to obtain 25 values of the minimum film thickness along the line of action, shown in Fig. (17)

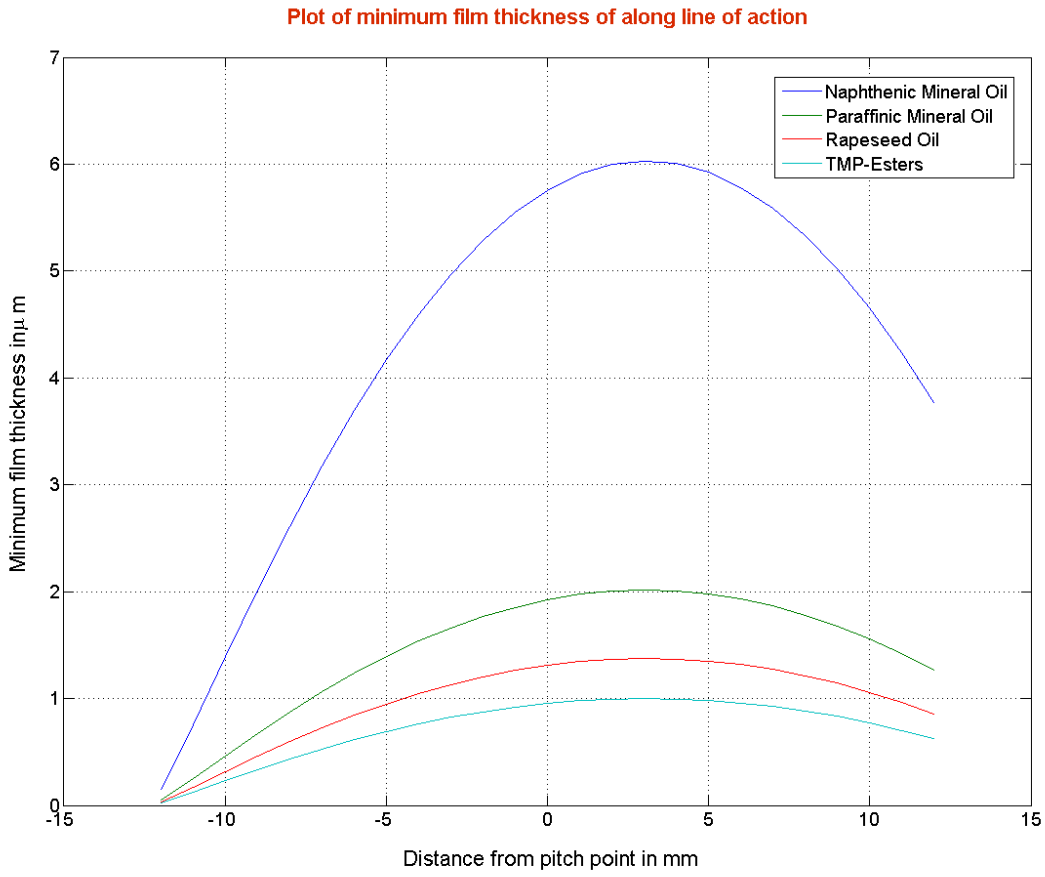

Figure 16, Plot of the minimum film thickness along profile direction only

The following correlation can be deduced from this case; the higher the pressure-viscosity co-efficient of the lubricant, thicker is the formation of the film. The film thickness of naphthenic mineral oil is considerably higher than that of the other three lubricants. But naphthenic mineral oil also has a very high value of the limiting shear-stress pressure co-efficient, which increases the friction. Therefore, a better alternative is rapeseed oil, which has the ability to form a thicker film as well as having low friction. Moreover, tests conducted at the Luleå University of Technology showed that systems using rapeseed oil run at a lower temperature; the risk of pitting is also reduced if a polyalphaolefin is used instead of naphthenic oil (Höglund, 1999).

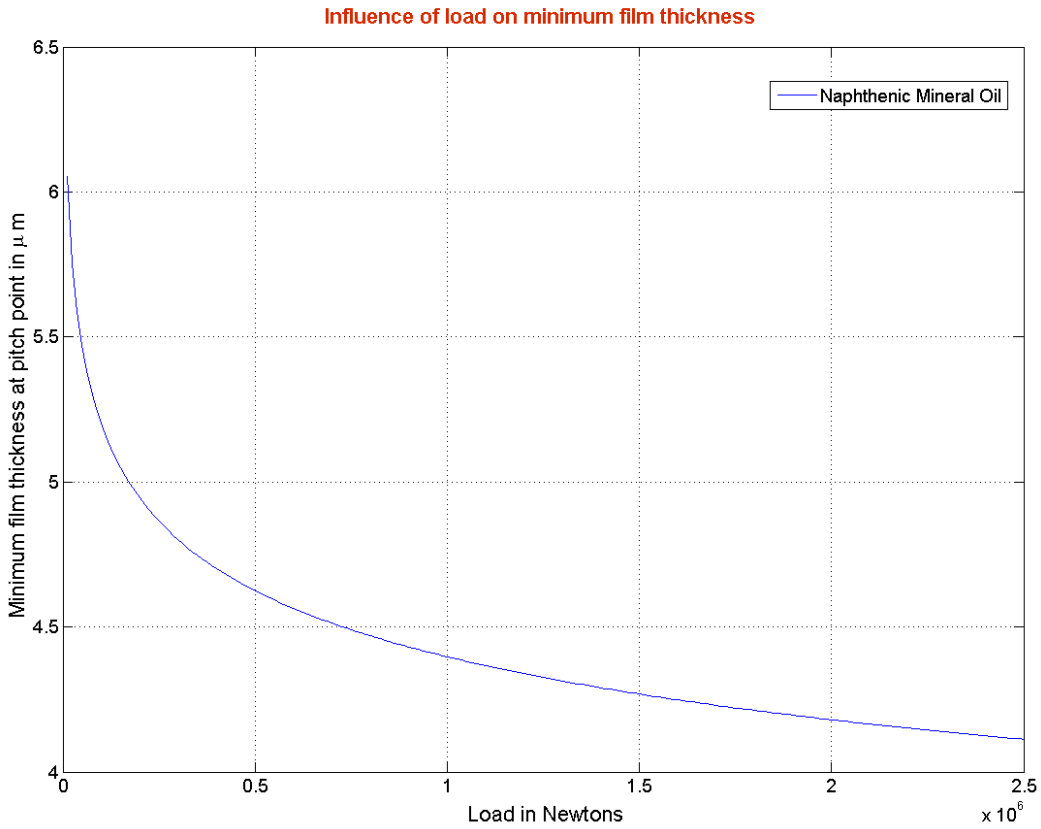

Figure 17, A plot demonstrating the influence of load on the minimum film thickness

In order to see the influence of load on the film thickness (Fig. (17)), the contact load was varied from 0 to 2.5 MN and correspondingly the film thickness was determined at the pitch point.
It can be observed that the effect is very minimal, for a load variation of 2.5MN, the change in film thickness is just 2µm. The plot in Fig. (18) shows the effect of the speed on the film thickness.
This agrees with Dowson et al., who state that the film thickness is little affected by the load and dependent on the speed. The load, however, affects the pressure distribution significantly.

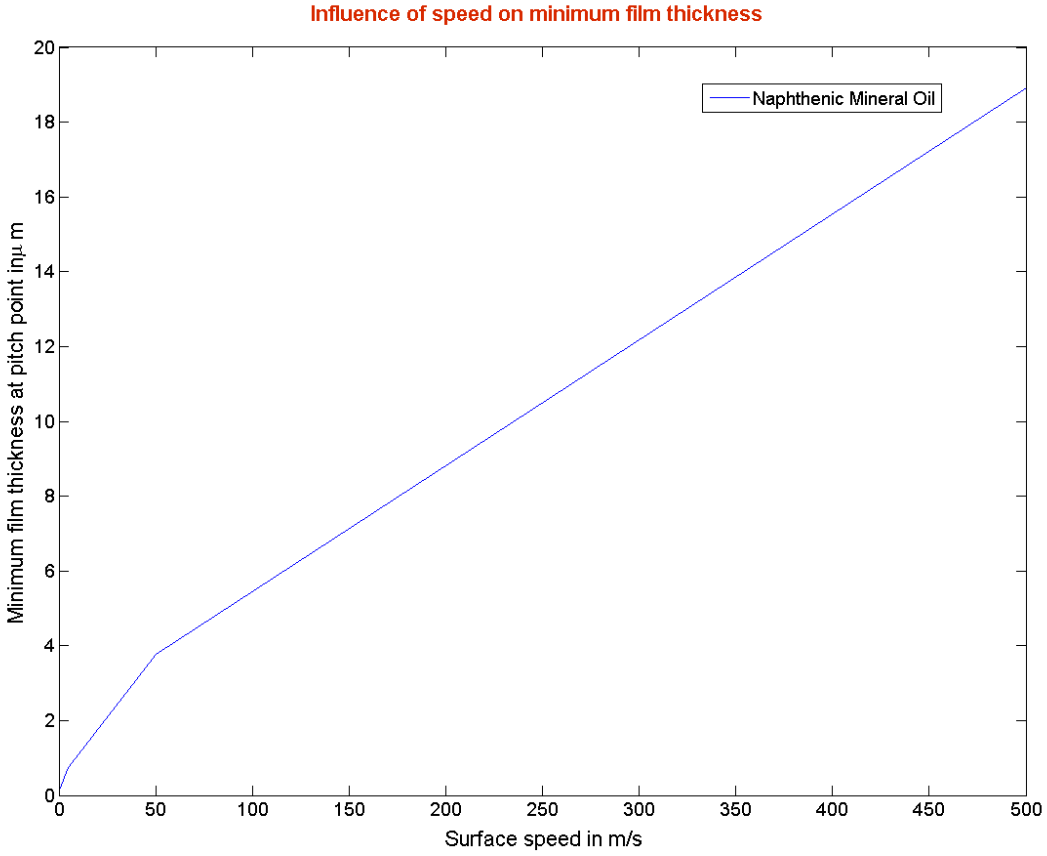

Figure 18, Plot demonstrating the effects of speed on film thickness

4.2 Results (Ordinary Spur Gear)

Helical 3D was now introduced and the methodology described in Chapter 3 was followed for calculating the minimum film thickness along the profile and face of the spur gear tooth. From here on, the implementation was carried out on only one lubricant, i.e. mineral oil, assuming an inlet temperature of 40^{o}C.

4.2.1 Minimum film thickness

The Fig. (19) shows a plot of the minimum film thickness on the pinion surface.

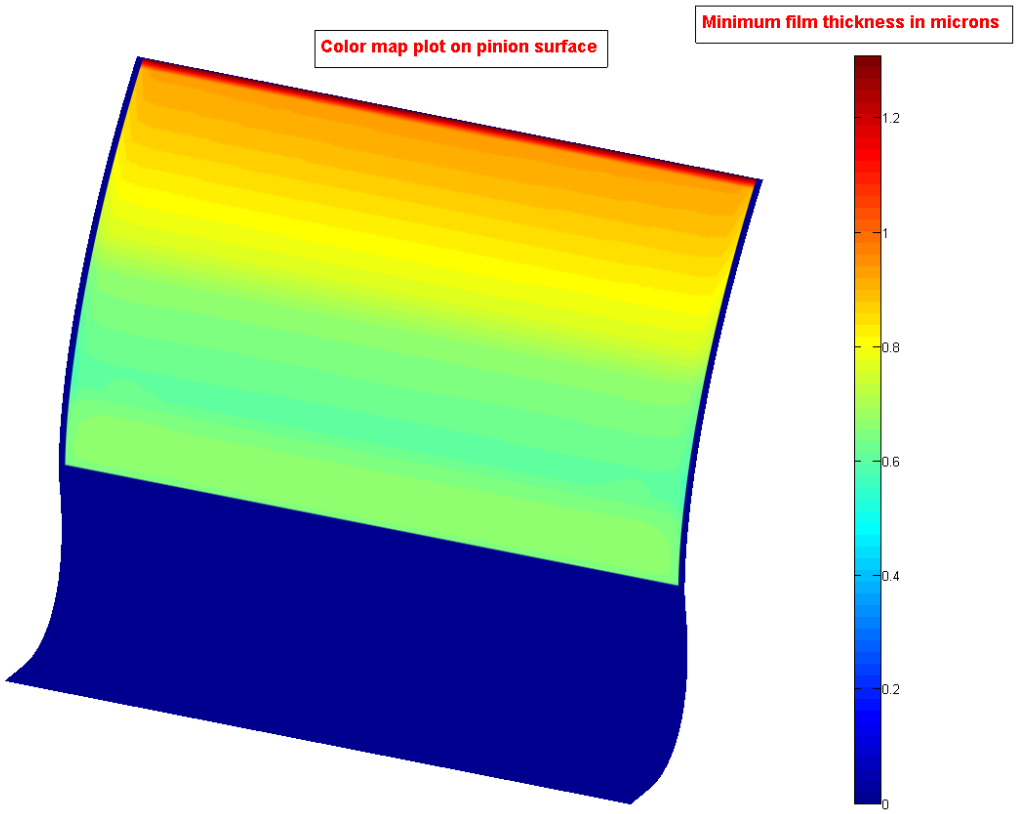

Figure 19, Minimum Film Thickness plot on pinion surface

Note that the film thickness is calculated for a contact, so the same color map will also be present on the mating gear surface.
The minimum film thickness is highest at the tip and lowest at the root. The maximum value is 1.32µm and the minimum is 0.57 µm. The centre line and surface plots illustrate more clearly the variation along the profile. From the above plot it can be seen that there is no variation across the face width of the pinion.
If only the centre line is considered, as shown in the Fig. (20), then the variation along only the profile can be seen more clearly.

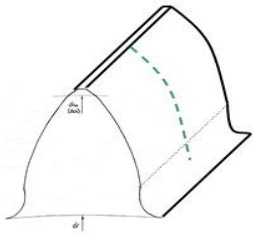

Figure 20, Centre line on gear tooth

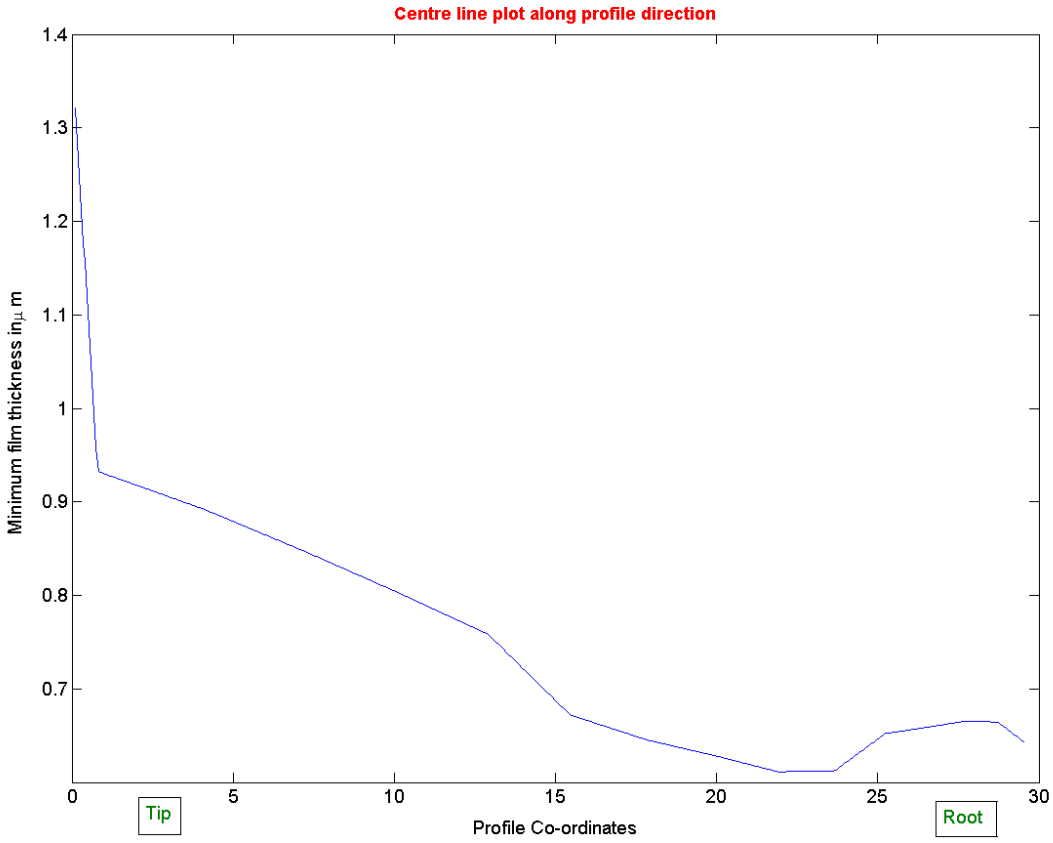

Figure 21, Plot of film thickness along centre line

The film thickness decreases steadily from tip to root. In general, the values are much lower in this case when compared to the simplest EHD model. There is also a significant change in the way the film thickness is distributed.

The Fig. (22) shows the minimum film thickness along the profile direction with and without the influence of the sliding velocity. The values are higher as a result of the occurrence of sliding. This is because the inclusion of the sliding velocity term increases the resultant velocity, and it was shown earlier as to how the minimum film thickness shares a directly proportional relationship with the velocity.

Note: Shear heating of the lubricant takes place as a result of the sliding, and this increases the temperature which reduces its viscosity, and thereby results in a decrease in the film thickness (Dowson, 1966). This thermal effect is included at a later stage.

4.2.2 Contact load per unit length

The highest values of the contact loads are observed in the pitch point region. There is a slight variation across the face width, with relatively higher values being present at either ends.

The lowest value is at the tip, as very little contact occurs there. Related plots can be found in appendix D.

4.2.3 Resultant Velocity

Higher values at the root and tip and comparatively lower values in the pitch point area.

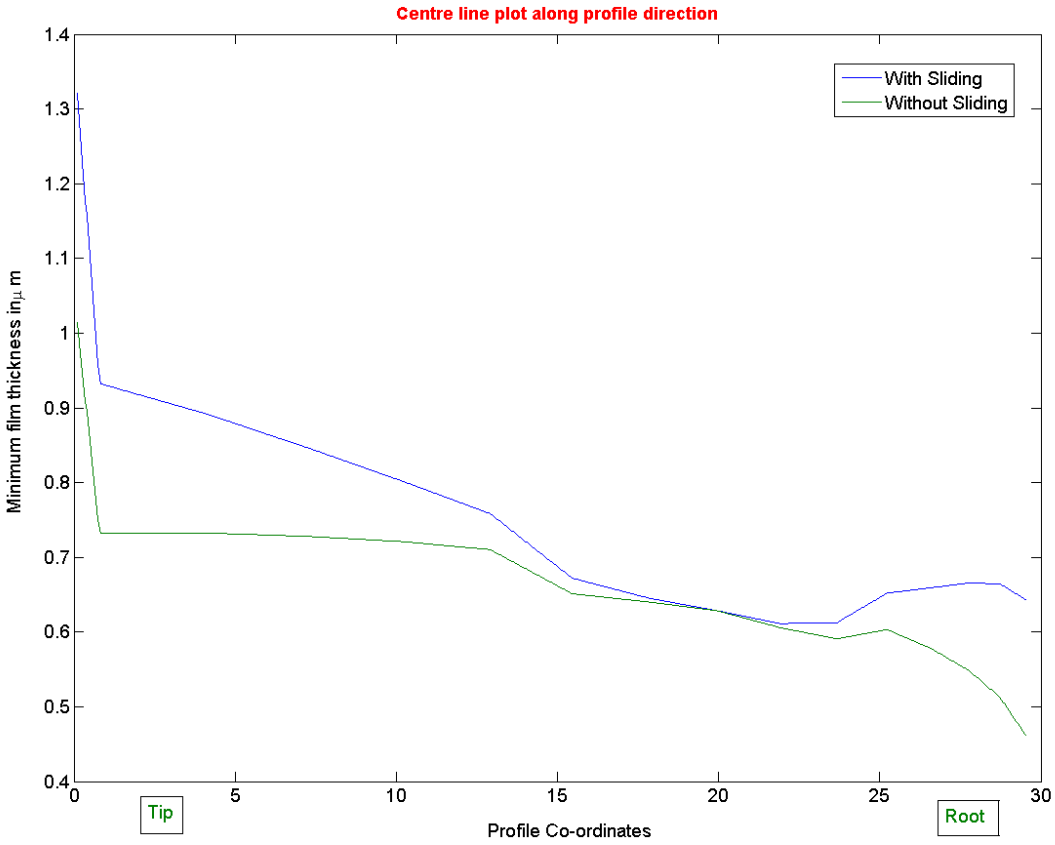

Figure 22, Plot of film thickness showing influence of sliding velocity

4.3 Spur Gear with Linear Tip Relief Modification

A linear tip relief modification was applied on both gear and pinion surfaces in order to investigate the behavior of the film thickness in that specific area. The details of the linear tip modification are shown in the Fig. (23).

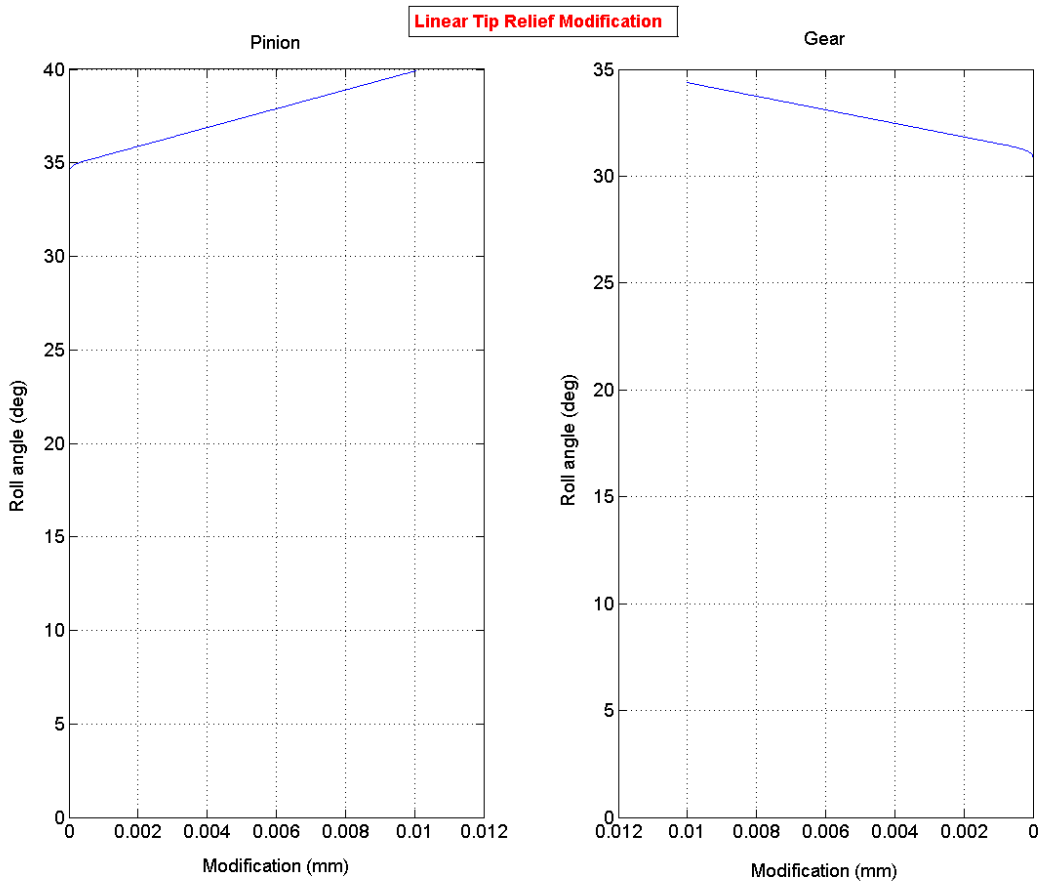

Figure 23, Details of linear tip relief modification on spur gear

4.3.1 Minimum film thickness

The Fig (24) shows a plot of the film thickness.

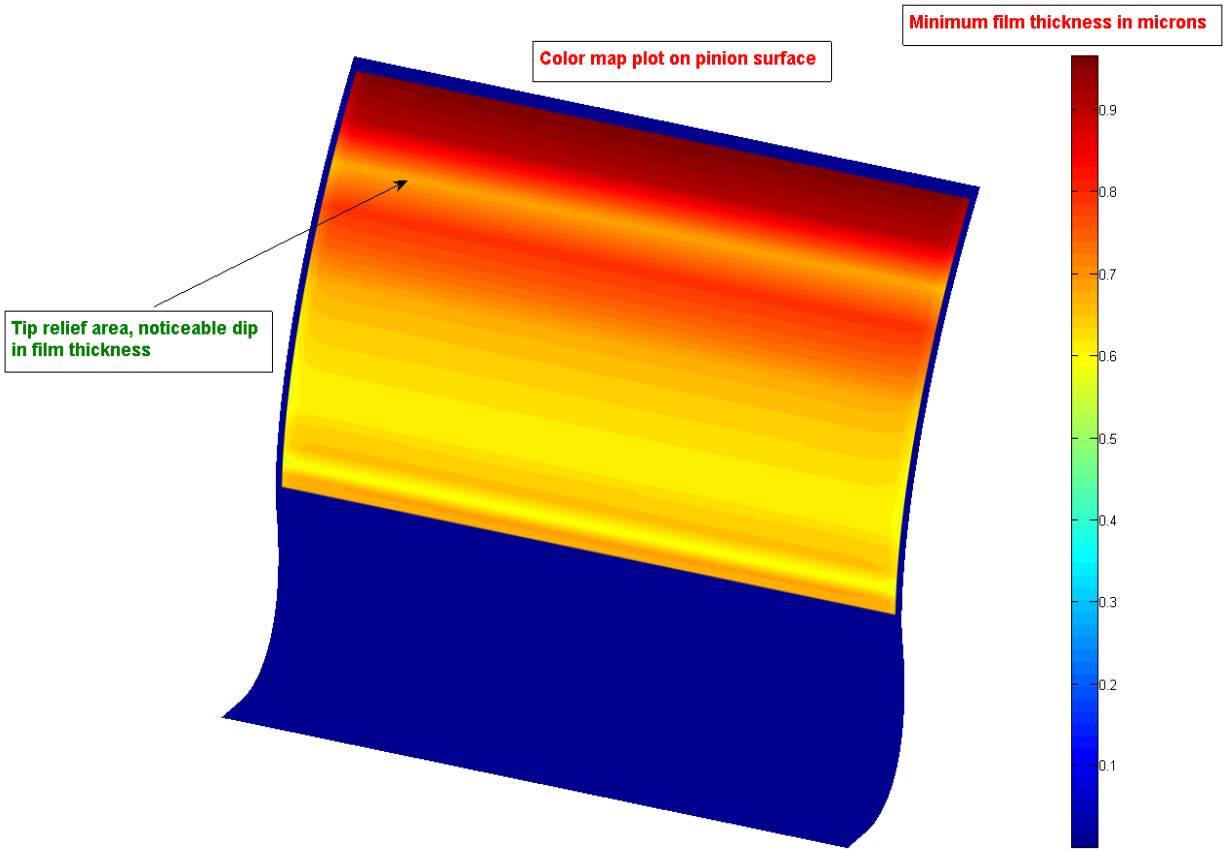

Figure 24, Influence of Linear Tip Relief

From the Fig. (24) it can be clearly observed that there is a decrease in the film thickness in the tip relief region. The magnitude of this decrease can be more clearly observed in a centre line plot shown in the Fig. (25).

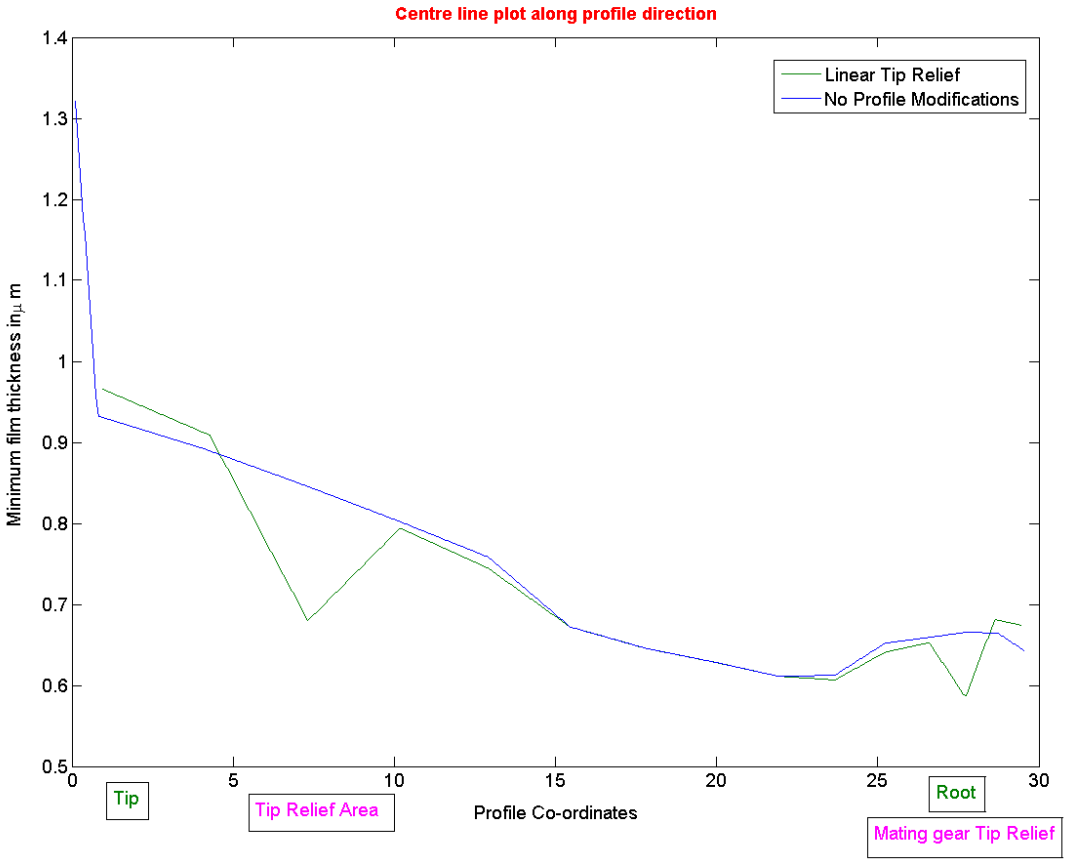

Figure 25, Centre line plot illustrating the effect of linear tip relief

The maximum amount of decrease in the film thickness was 0.2μm. This difference continued to increase as more amount of material was removed. The tip relief region is like a sharp corner; the decrease in the relative radius of curvature and speed contributing to the effect of the film thickness being lowered. There were no observable changes in the contact load.

4.3.2 Relative Radius of Curvature

The relative radius of curvature shows a sharp decrease in the tip relief region. Refer to plot in appendix D.

4.4 Spur Gear with Quadratic Tip Relief Modification

A quadratic tip relief modification (details in Fig. (26)) was applied on both gear and pinion surfaces; the Figs. (27) and (28) show the behaviour of the film thickness in the tip relief region.

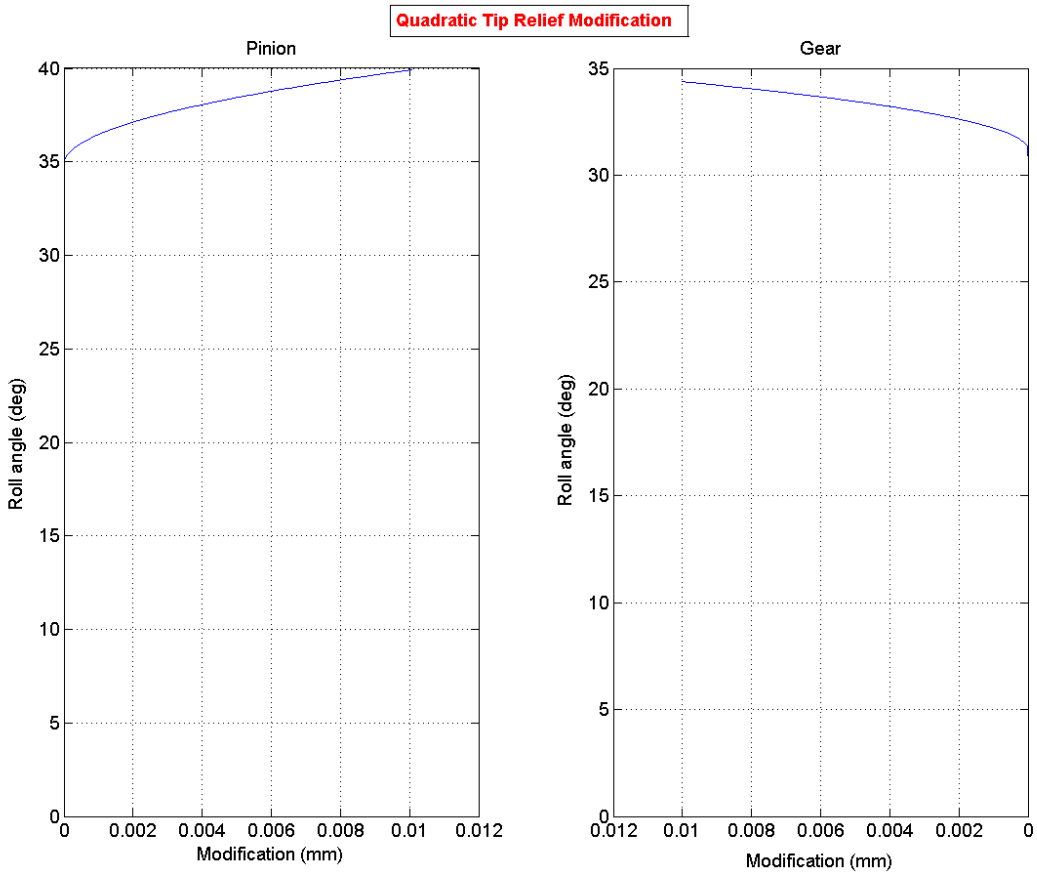

Figure 26, Details of quadratic tip relief modification on spur gear

4.4.1 Minimum film thickness

The Fig. (27) shows a plot of the film thickness on the pinion surface.
Fig. (28) more clearly illustrates the variation in film thickness by also making a comparison with the earlier cases of no modification and a linear tip relief modification.
The maximum reduction in film thickness is 0.05µm and a smooth transition can be observed along the region.
The scope for wear is more in the tip relief region, therefore the ideal scenario would be to avoid the tip relief itself. However, the application of a tip relief offers other advantages such as noise reduction and a smoother operation when the teeth come into engagement. Therefore it is advisable to use a quadratic tip relief as demonstrated since the reduction in film thickness is significantly lower when compared to a linear tip relief modification. Lesser amount of material removal and a higher corner radius would bring about a much smoother transition in the tip relief region and thereby reduce the scope for wear; achieving this is however difficult from a manufacturing perspective.

The variations in the speed and relative radius of curvature are very slight, unlike the case of the linear tip relief modification (refer to plots in appendix D).

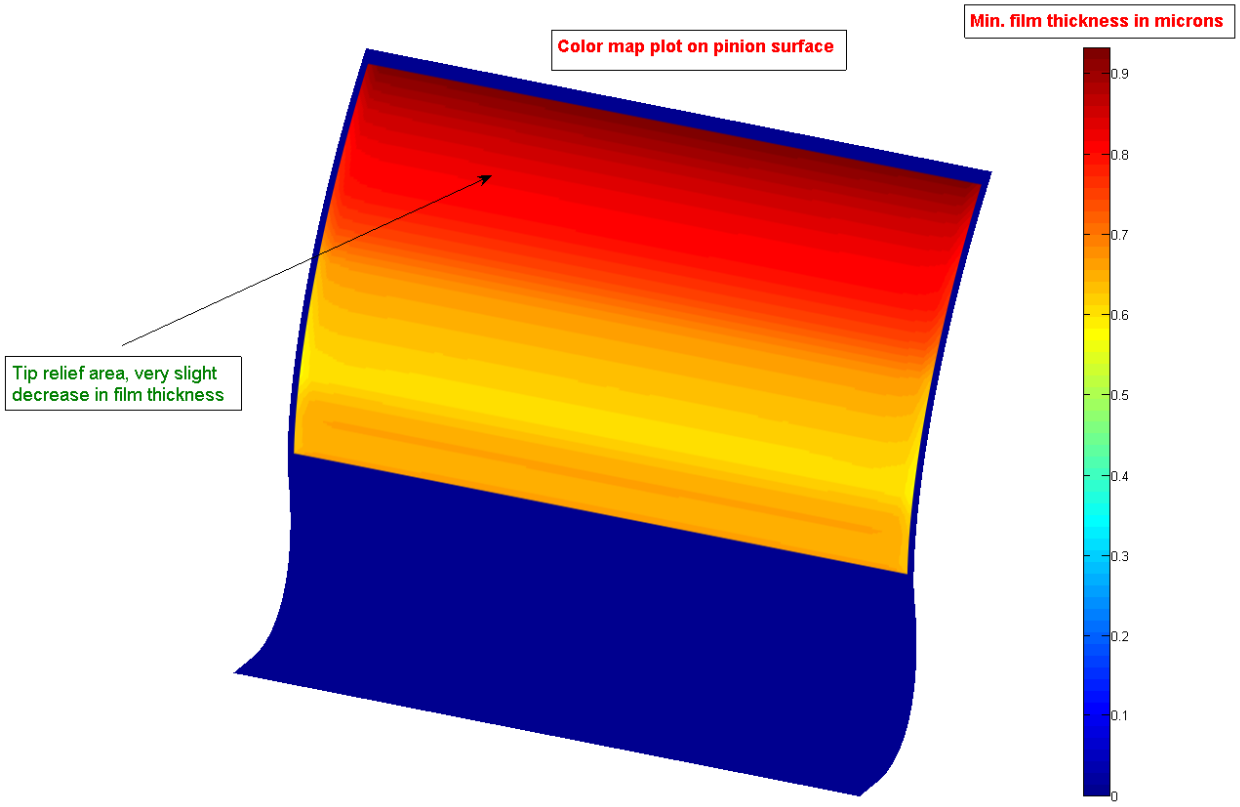

Figure 27, Influence of quadratic tip relief

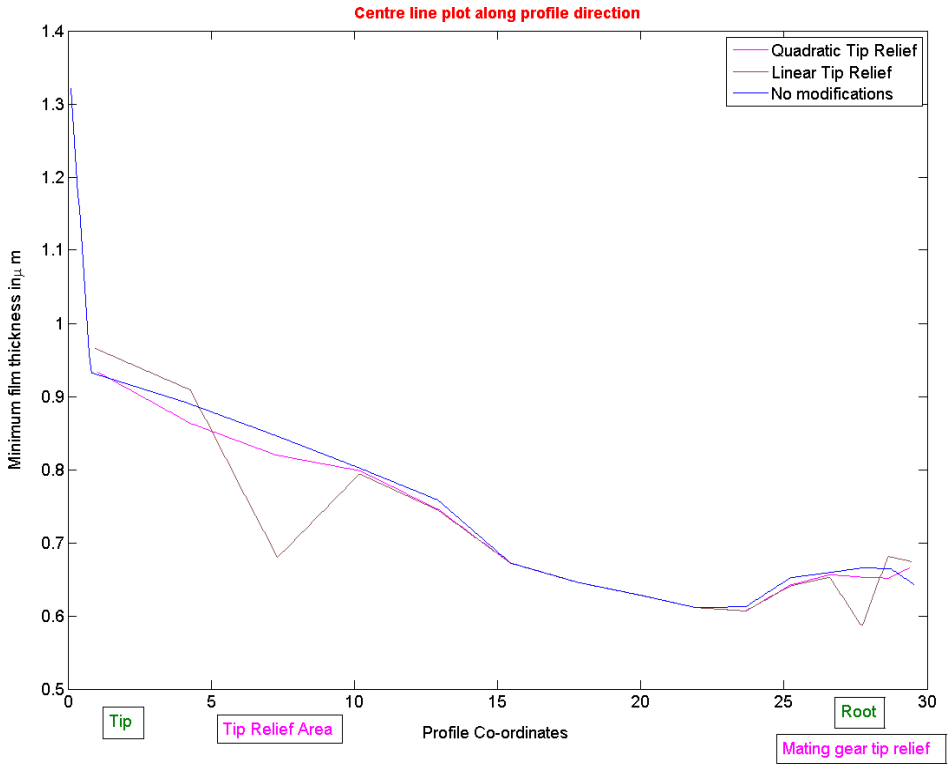

Figure 28, Comparison of all the three cases

4.5 Spur Gear with Tip Relief Modification and Thermal effects

The thermal correction factor was determined from the equations specified in section 2.9. The new value of the film thickness was obtained by multiplying this factor with the present value:

$$h_{\min(thermal)} = h_{min} \text{ x } C_t \quad (26)$$

The centre line plot in Fig. (29) illustrates the influence of the thermal effects more clearly:

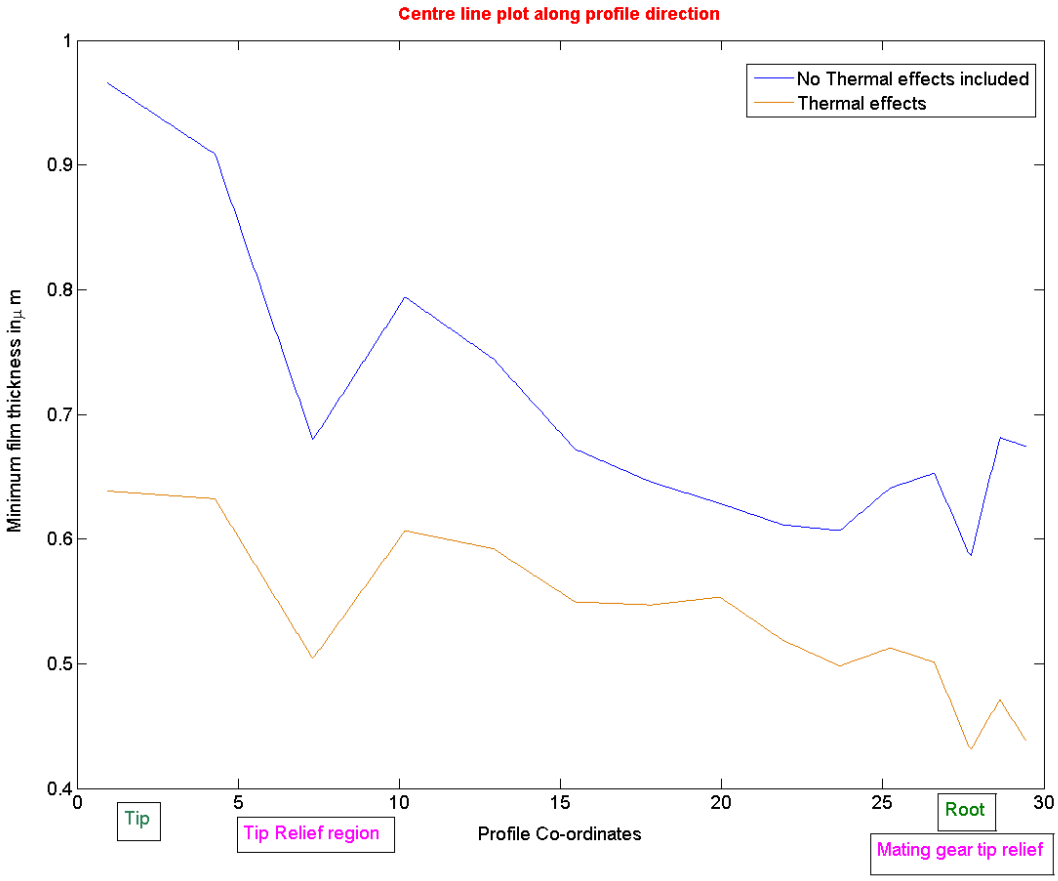

Figure 29, Plot illustrating the influence of thermal effects (linear tip relief)

There is a significant proportional reduction in film thickness owing to the thermal effects. There is a reduction in film thickness in the tip relief region also in the presence of thermal effects.
The average percentage reduction in film thickness was calculated as 24.79%.
Similar trends were observed (Fig. (30)) even in the case of a quadratic tip relief modification being applied.

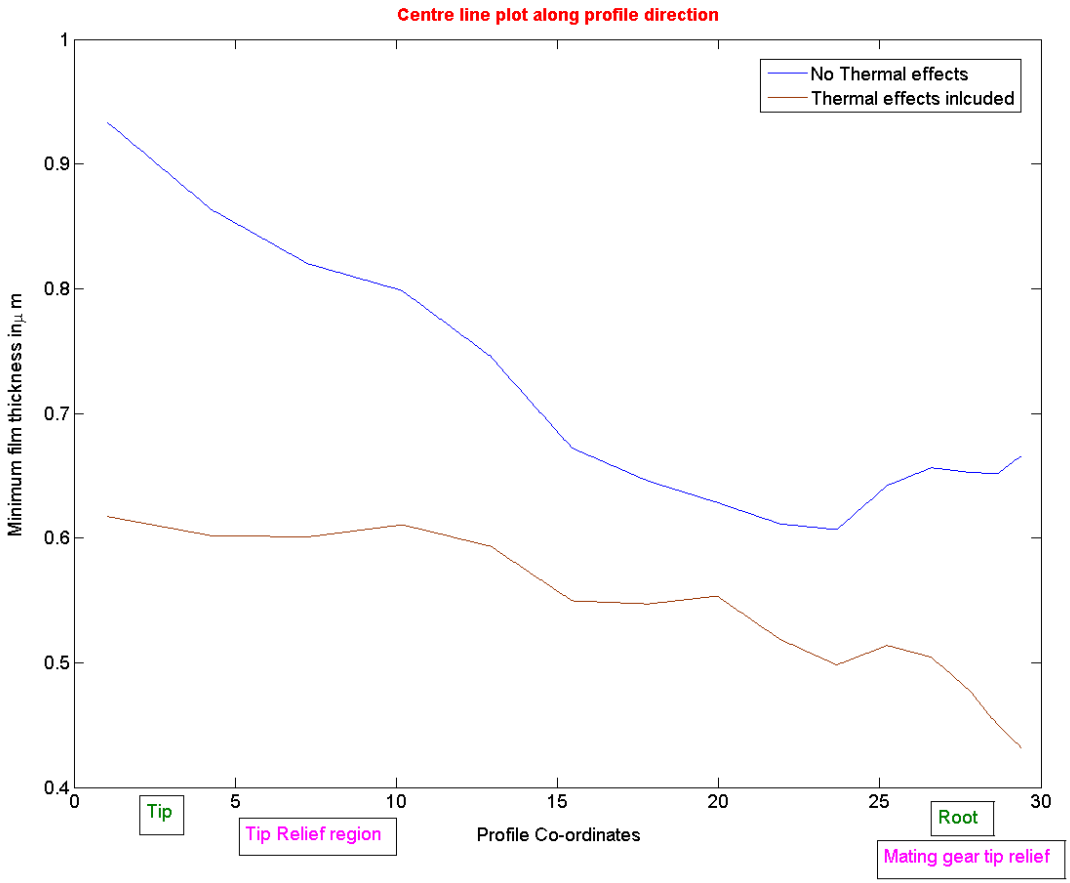

Figure 30, Plot illustrating the influence of thermal effects (quadratic tip relief)

4.6 Roughness parameter (Spur gear models)

As stated in section 2.10, values for the film thickness were determined for perfectly smooth surfaces. The roughness parameter was used to determine the lubrication regime for all the various spur gear models mentioned earlier.

For all the various models, the average value of the minimum film thickness was calculated and substituted in (12) to determine the roughness parameter Λ. The lubrication regime was thereby determined from Table (1). This was done for four different finishing methods; the values of the composite rms roughness were taken from (Gohar, 2001):

The following Table (3) illustrates the lubrication regimes for different spur gear models; with **honing** as the method of surface finish. Refer tables in appendix E for various other surface finish processes.

Note that these values are for one particular standardized gear which is rotating at a specific rpm and with a fixed value of the input torque.
The influence of the thermal effects can be seen in certain situations; for example when the type of finish is lapping, for the case of the ordinary spur gear the mode of lubrication shifts from mixed to boundary when thermal effects are included.
Another important factor for determining the scope for wear is the type of finishing method that is employed. Moreover, gears that are run-in are better, since the surfaces become smoother after the running-in process, thus increasing the Λ value and thereby reducing the probability of film breakdown.

Table 3, Lubrication regimes for different spur gear lubrication models (honing)

Type of lubricant model	Lubrication regime
Ordinary spur-no thermal effects	Mixed
Ordinary spur-thermal effects	Mixed
Spur with linear tip relief (no thermal effects)	Mixed
Spur with linear tip relief and thermal effects	Mixed
Spur with quadratic tip relief (no thermal effects)	Mixed
Spur with quadratic tip relief and thermal effects	Mixed

4.7 Ordinary Helical Gear

The next part of this thesis focuses on helical gears. In chapter 2, it was stated that the contact between two spur gear teeth can be represented by two cylinders. The contact is a nominal straight line contact and therefore, the formula of the minimum film thickness could be safely applied (formula uses contact load per unit length). In the case of the helical gear however, the contact is not a nominal straight line contact along the face. But since a finite element approach is being used here with the contact zone being divided into a number of tiny grid cells, it would be safe to assume the contact between two grid cells (pinion and mating gear) as a nominal straight line contact.
This assumption is based on the following logic: An arc or a curve is represented as a summation of a number of differential straight line segments, similarly in the case of the helical gear, the curved face can be seen as the summation of very tiny rectangular grid elements.
Initially, simulations were done on an ordinary helical gear without any profile modifications. From appendix A, it can be seen that there is a considerable difference in the input torque when compared to the spur gear.
Parameters such as friction co-efficient, flash temperature and losses were determined for the fairly complex and realistic model, i.e., a helical gear with profile modifications and thermal effects.

4.7.1 Minimum film thickness

The film thickness distribution on an ordinary helical gear without any profile modifications is shown in the plots in Figs. (31), and (32).

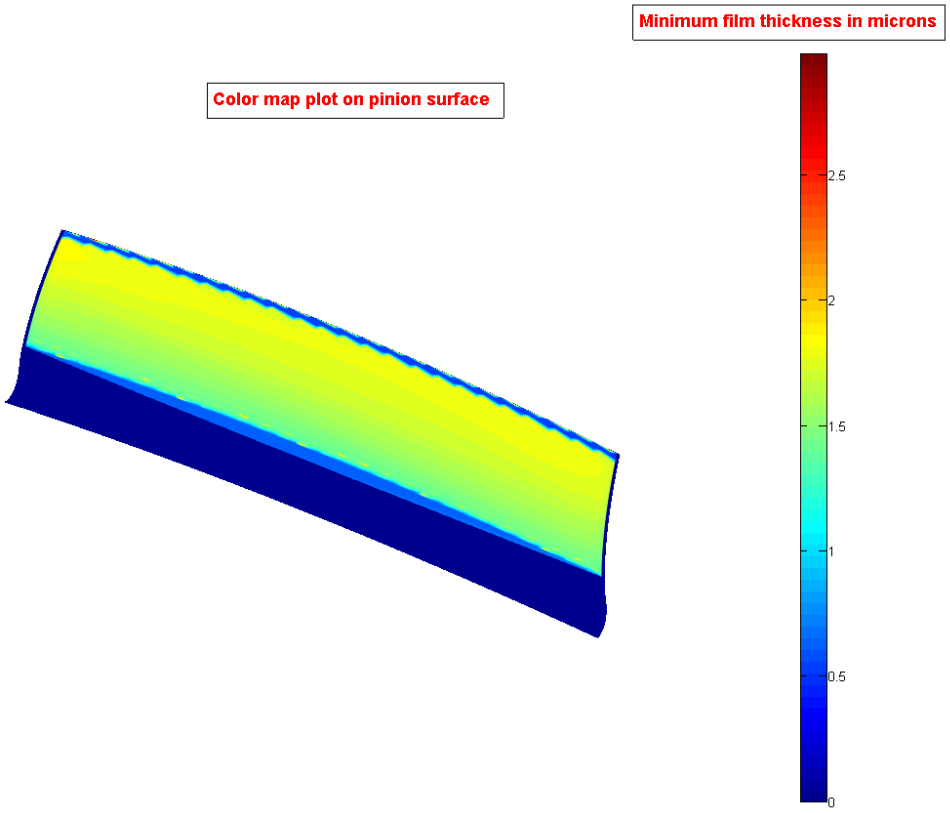

Figure 31, Plot of minimum film thickness on pinion surface

The average value of the film thickness is 1.54 µm, and the minimum and maximum values are 0.48 µm and 3.37 µm respectively. The difference between these values is much higher when compared to a spur gear, which shows that the variations in film thickness can be quite significant in a helical gear.
The surface scatter plot shown in appendix illustrates the variations in film thickness along the face of the pinion; there had been very little or almost zero variation along the face for the spur gear. The reason for this is the relative changes in contact area along the helical gear face.

From the plot shown in Fig. (32), it can be seen that the film thickness is steady at around 1.7 µm along most of the profile, except for a big bump at the very tip. This could be attributed to the very low contact area at the beginning of the engagement in the case of a helical gear.
A low contact area also represents a low relative radius of curvature, illustrated in Fig. (33).

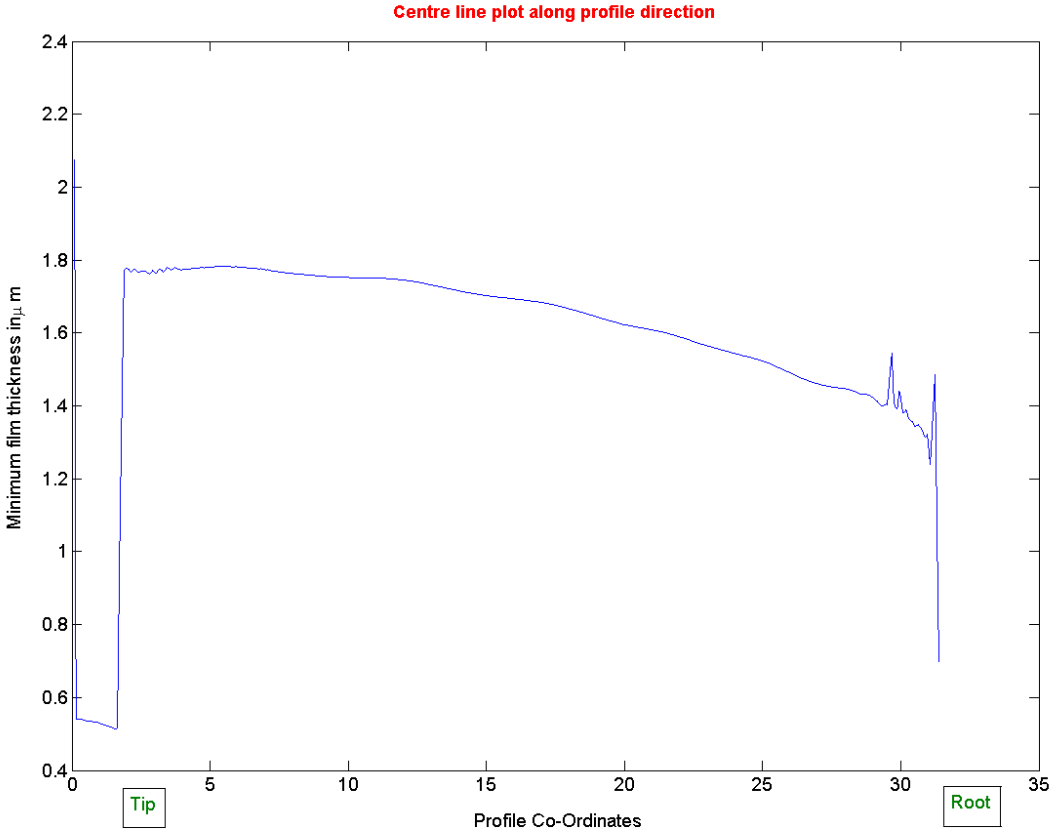

Figure 32, Film thickness plot along centre line

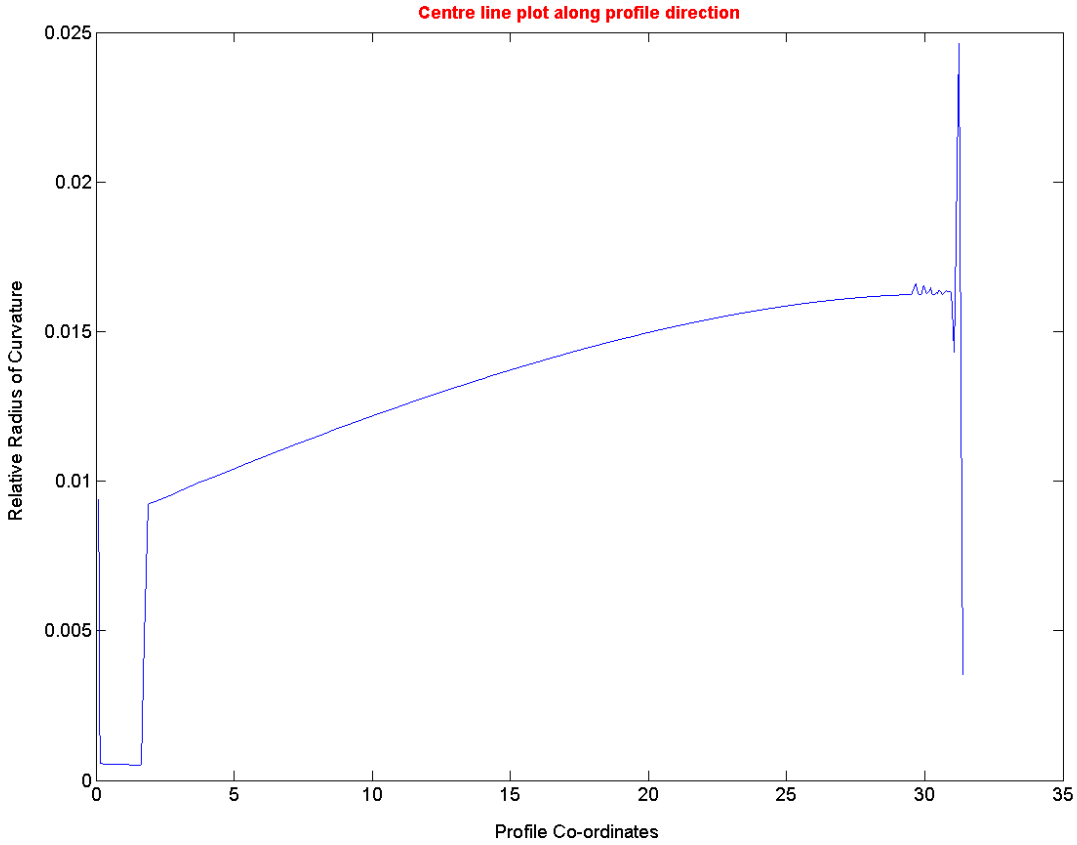

Figure 33, Relative Radius of Curvature plot along centre line

4.8 Helical Gear with Modifications

When profile modifications (tip relief, lead and profile crowning), shown in Fig. (34), were applied on the helical gear and a plot of the minimum film thickness was obtained using the normal approach, it was observed that there was actually an increase in the film thickness in the tip relief area.

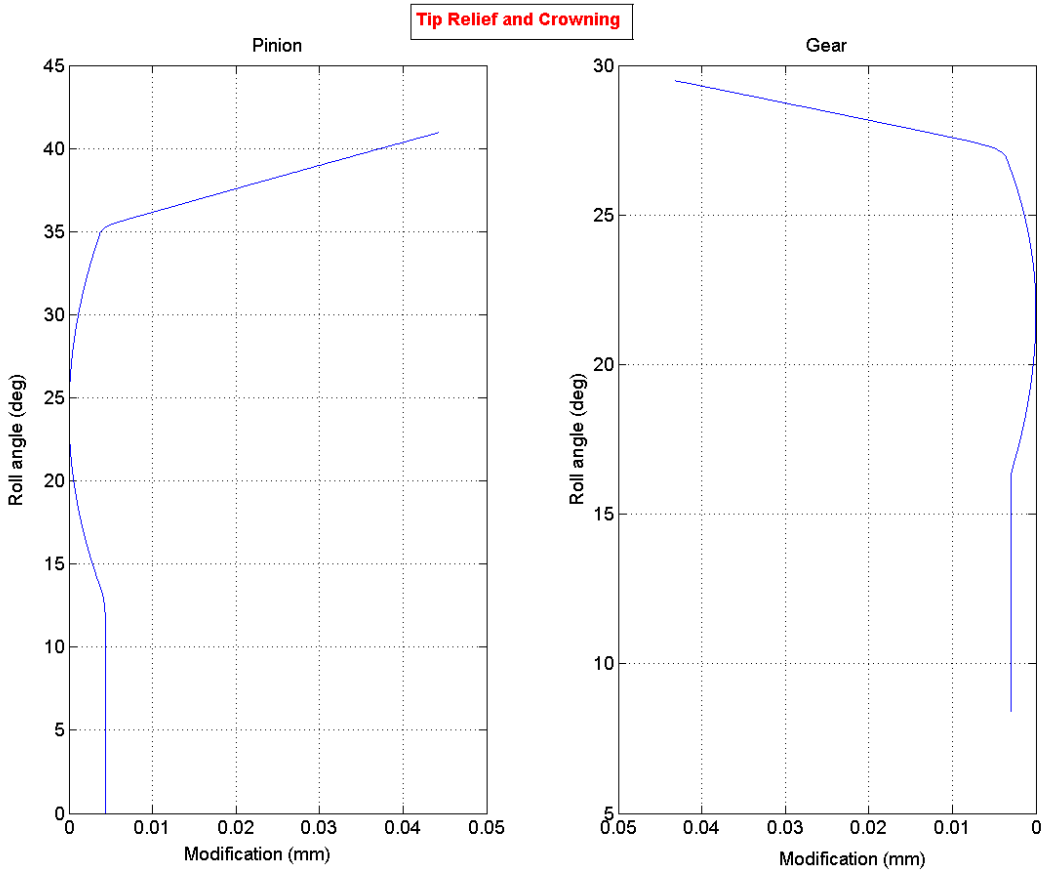

Figure 34, Details of modifications on helical gear

This was attributed to an improper calculation of the velocities in the tip relief region by Helical 3D; so the velocities were obtained in a different manner than directly extracting the values from the program. This was done using the conventional linear velocity equation (formulae taken from (Dudley, 1984)).

$$V = R\omega \tag{27}$$

where R is the distance vector and ω is the angular velocity.
The distance vector is calculated separately for both gear and pinion.

$$R_{pinion} = R_{pitch(pin.)} sin\psi_s - s_{pin.} \tag{28}$$

$$R_{gear} = R_{pitch(gear)} sin\psi_s - s_{gear} \tag{29}$$

The values of the s vector are obtained from helical 3D.
The rolling velocity is determined as:

$$RV_{pinion} = R_{pinion}\, x\, \omega_{pinion} \tag{30}$$

$$RV_{gear} = R_{gear}\, x\, \omega_{gear} \tag{31}$$

The combined rolling entrainment velocity:

$$RV_{combined} = \left(\frac{RV_{pinion} + RV_{gear}}{2}\right) \tag{32}$$

The resultant velocity takes into account the sliding component as well:

$$V_{resultant} = \sqrt{RV_{combined}^2 + \left(RV_{pinion} - RV_{gear}\right)^2} \tag{33}$$

The angle ψ_s is known as the transverse working pressure angle and is determined in the following manner for a helical gear.
Refer to the appendix for helical gear data
The normal pitch diameter of the pinion is calculated as:

$$P.d._{pinion(n)} = \frac{2Ga}{G+1} \tag{34}$$

where

G is the gear ratio
a is the center to center distance in mm
Substituting from (appendix A), this value is obtained as:

$$\mathrm{P.d._{pinion(n)}} = 96.96\mathrm{mm} \tag{35}$$

Similarly, for the gear,

$$\mathrm{P.d._{gear(n)}} = 203.03\mathrm{mm} \tag{36}$$

Next, the base diameters of the gear and pinion are calculated:

$$B.d._{pinion} = \frac{Zm\cos\tau}{\cos\beta} \tag{37}$$

where

Z is the number of teeth
m is the module
β is the helix angle in radians

τ is the pressure angle in radians
The values are obtained as:

$$\text{B. d.}_{\text{pinion}} = 89.75\text{mm} \tag{38}$$

$$\text{B. d.}_{\text{gear}} = 206.43\text{mm} \tag{39}$$

Finally, the transverse working pressure angle ψ_s found out from the following equation:

$$cos\psi_s = \frac{B.d._{pinion} + B.d._{gear}}{2a} \tag{40}$$

$$\psi_s = 22.24^o \tag{41}$$

Using the new velocities calculated from (30) and (31), the minimum film thickness obtained is shown in Fig. (35).
Note the decrease in film thickness in the tip relief region. Like the earlier case of the spur gear, a comparison has not been made between linear and quadratic tip relief since this is a standard profile modification used by Scania CV AB and it was not in the requirements of the thesis to investigate the influence of varying profile modifications.
The minimum and maximum values of the film thickness are are 0.56 µm and 3.59 µm respectively. Like the earlier case, some variations along the face can also be seen. (refer to surface plot in appendix D.)
The lowest values of the contact load are at the extremities and the maximum values are present near the pitch point region.
High values of the resultant velocity are observed at the tip; also the dip in the speed in the tip relief area can be seen from the above plot. The centre line plot shows a steady linear decrease in the speed from the tip to the root. (refer in appendix D).

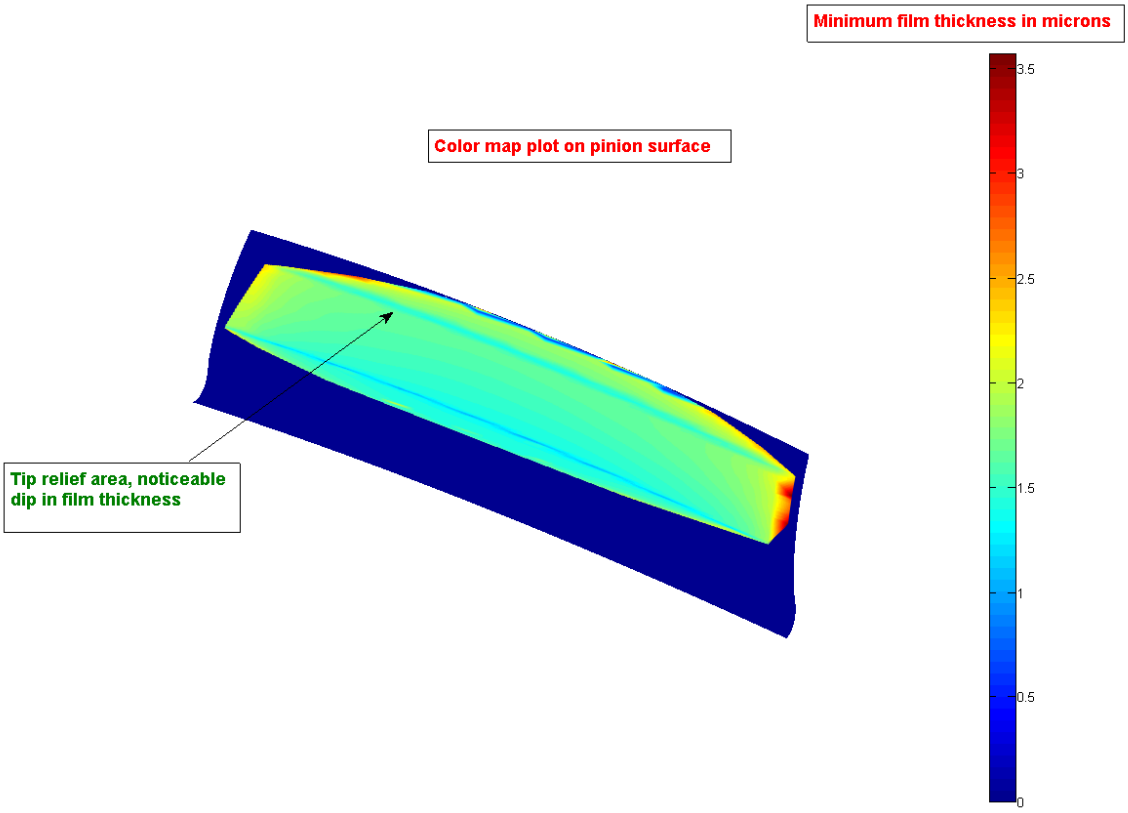

Figure 35, Plot of film thickness with the inclusion of profile modifications

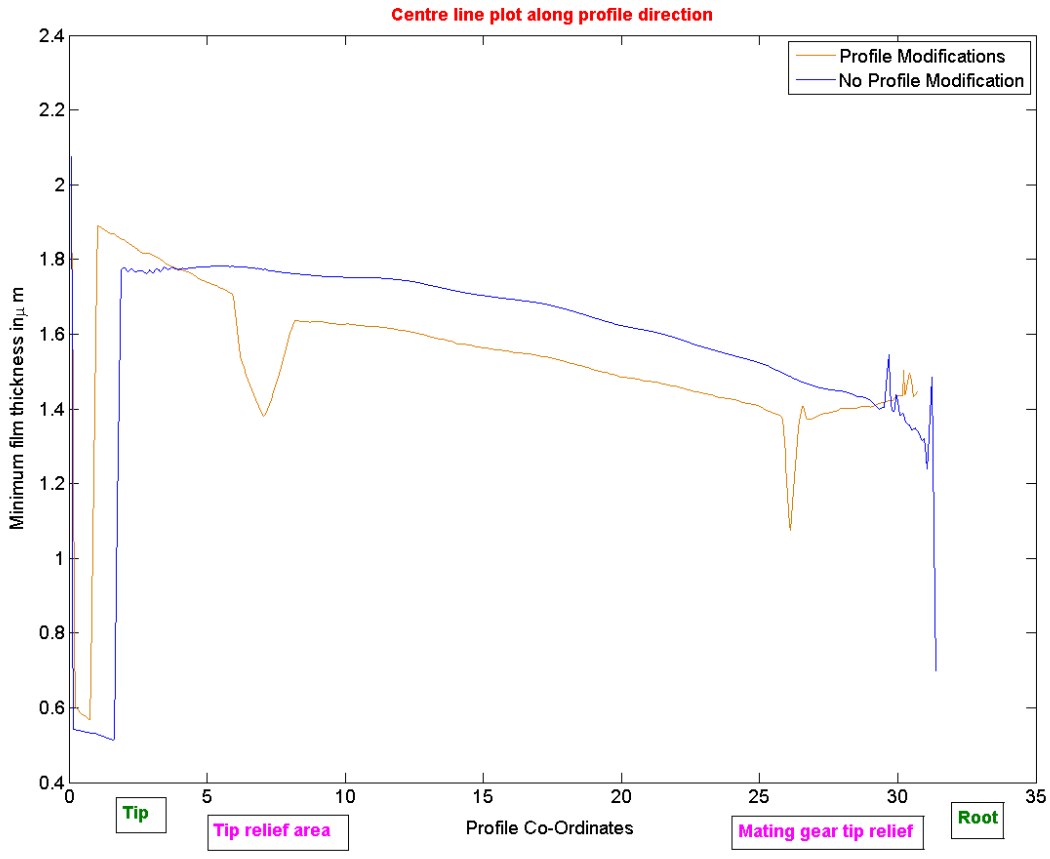

Figure 36, Centre line plot showing effect of modifications

4.9 Helical Gear with Modifications and Thermal effects

With the inclusion of thermal effects in the model, this becomes the targeted realistic model.

4.9.1 Minimum film thickness

The Fig. (37) shows a plot of the film thickness:

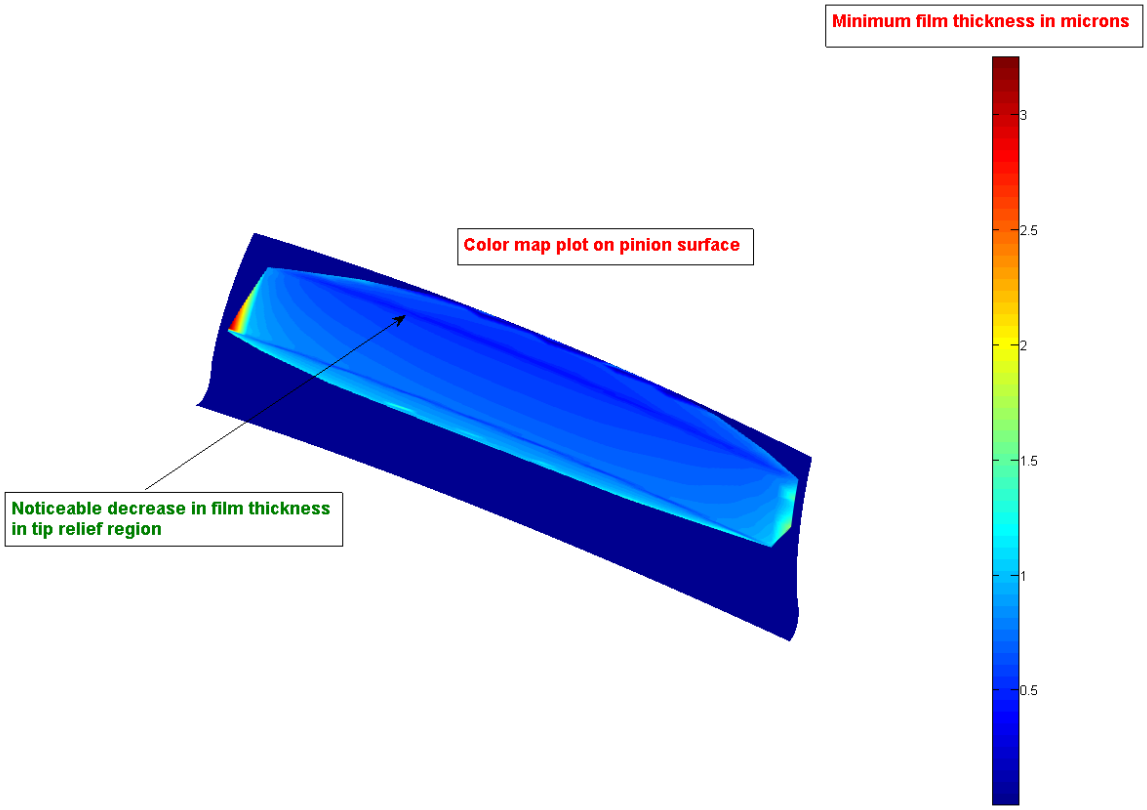

Figure 37, Plot of film thickness on helical gear surface with modifications and thermal effects

The average value of the film thickness was 0.67 µm; a percentage reduction of 56.49% when compared to the previous model without any thermal effects. The plot in Fig. (38) illustrates this comparison more clearly. The decrease in film thickness in the tip relief region can be observed here also.

4.9.2 Friction Coefficient

The friction co-efficient was determined using (8) at various points along the profile and face of the helical gear tooth. Since smooth surfaces were assumed, the value of the surface roughness was taken as zero and substituted in the equation.
The plot in Fig. (39) shows the distribution of the friction co-efficient along the surface of the pinion. The average value is 0.06, with relatively lower values found at either ends of the face and higher values found along the pitch point region. This is surprising, since the rolling friction is much lesser than the sliding friction; and only pure rolling occurs in this area. Doubts with regard to the accuracy of the Benedict Kelly model in this region have been raised before in literature.

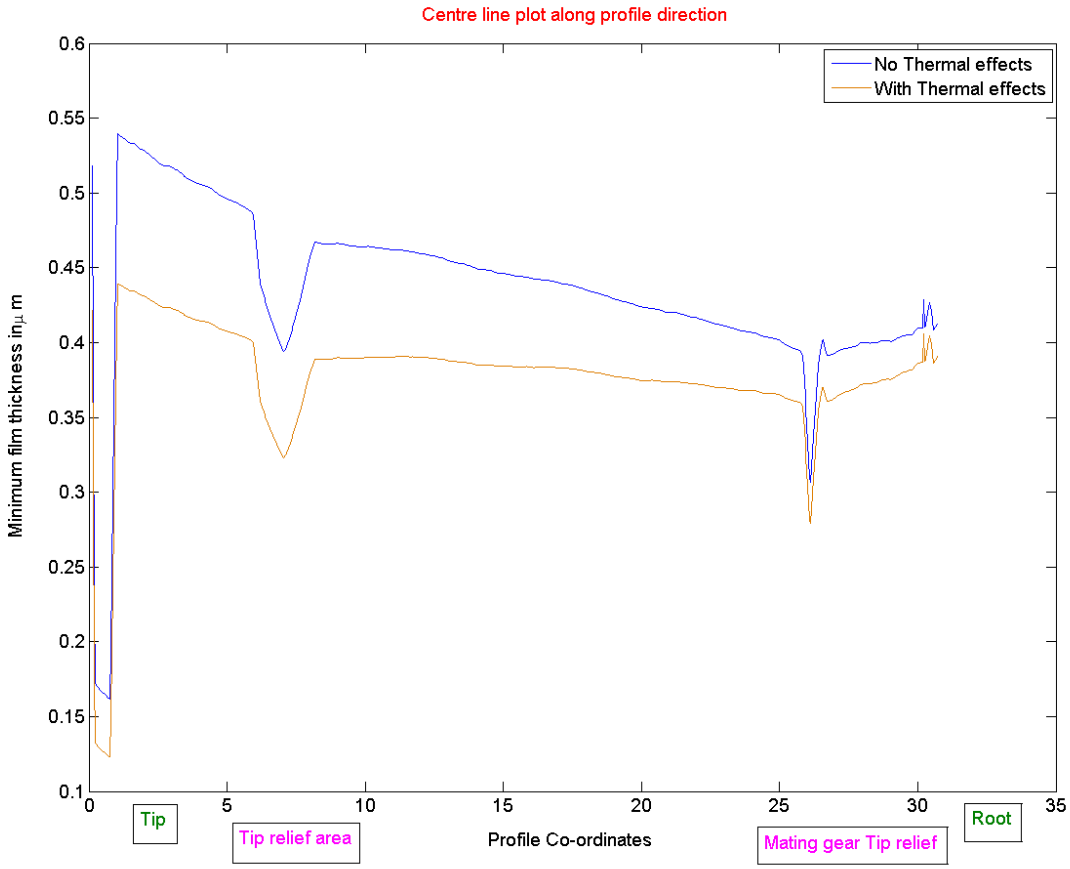

Figure 38, Influence of thermal effects

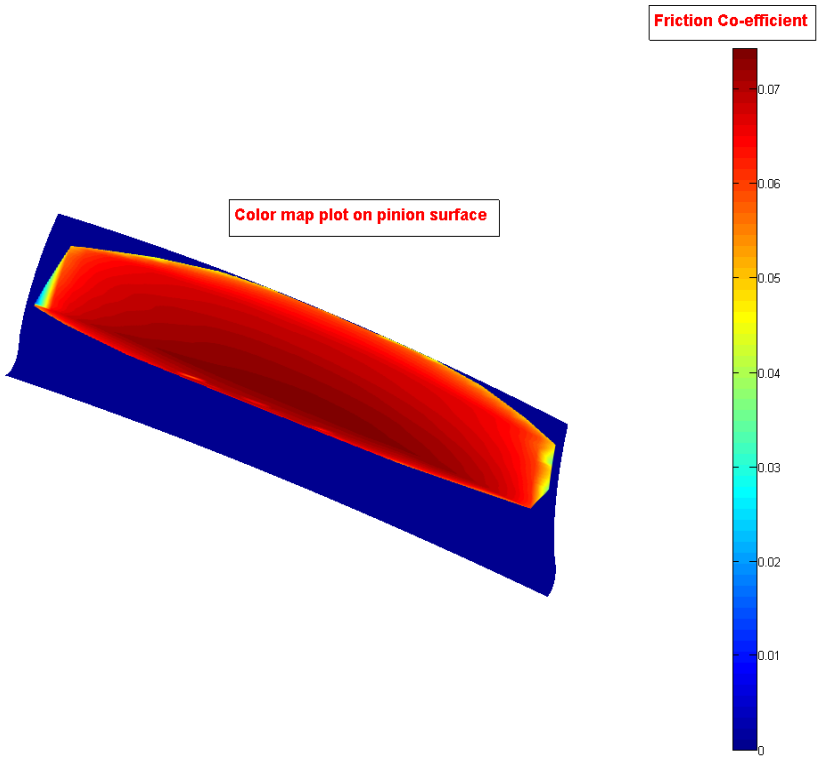

Figure 39, Plot of friction coefficient on pinion surface

4.9.3 Flash Temperatures

With the use of (7), the flash temperatures were determined at various points along the profile and face of the gear tooth. To these flash temperatures, the bulk temperature was added in order to obtain the contact temperature.
The distribution of flash temperatures is shown in Fig. (40).

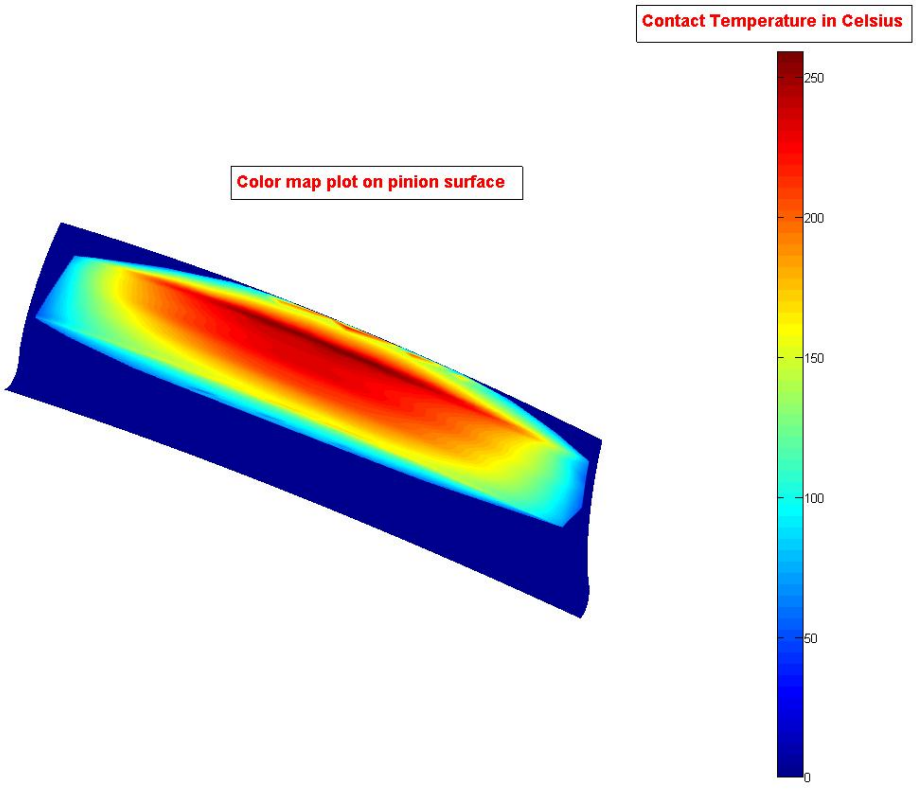

Figure 40, Plot of flash temperatures

The plot shows a considerable amount of variation along both profile and face. Along the face, lower values of the flash temperature are present at either ends. The contact temperature is 250 C (maximum) in the tip relief region. Lower values can be observed at the extremities, i.e. root and tip.

4.10 Roughness Parameter (Helical gears)

The roughness parameter was calculated for the various helical gear models in a manner similar to the one described in section 4.4.

Table 4, Lubrication regimes for different Helical gear models (honing)

Type of lubricant model	Lubrication regime
Ordinary helical-no thermal effects	Mixed
Ordinary spur-thermal effects	Mixed
Helical with modifications (no thermal effects)	Mixed
Helical with modifications and thermal effects	Mixed

As can be observed from the Table (4), for all possibilities, the lubrication regime is mixed, which is desirable. Other observations stated in section 4.4 apply to helical gears also.

4.11 Losses and efficiency

From (16), the tooth losses were calculated at all points of contact. The units are in watts.
The mean value of the losses was 7.21 Watts. The maximum losses occurred at the very tip and there was also a spike in the tip relief area.
The losses on the pinion surface are illustrated in Fig. (41).

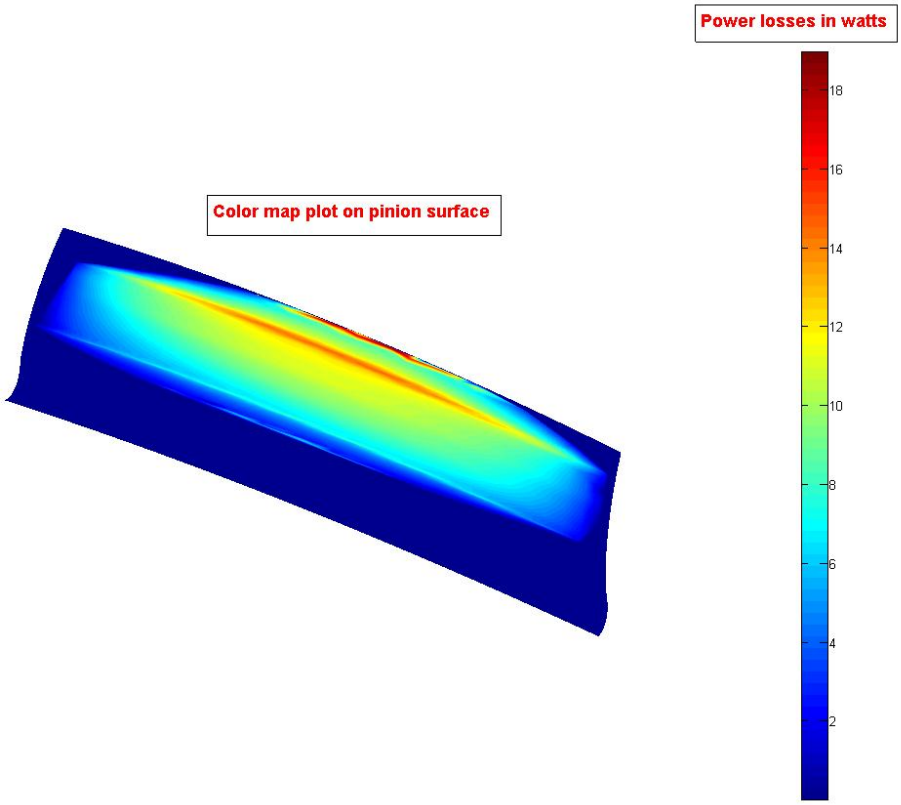

Figure 41, Plot of the tooth losses

In order to compute the instantaneous efficiency, (15) was slightly modified since it gave the efficiency at only one contact point. This, however, does not make sense since for each time step, contact occurs at a number of points (grid cells or load segments) and the losses need to be summed up for all these load segments in order to get the total actual value. The efficiency expression after modification is,

$$\eta_{eff.} = 1 - \sum_{q=1}^{Q} \left[\frac{\left| F_r + F_f \right|}{L_{in}\omega_{in}} \right] \tag{42}$$

where Q denotes the number of load segments (or grid cells) in this case. If the example provided in Chapter 3 is considered, then the value of Q would be 81. The rolling component is neglected, F_r=0.
In this manner, the efficiency was computed for all the twenty one time steps (for one mesh cycle) along the profile of the gear tooth. The input power in this case was:

$$L_{in}\omega_{in} = 1500 \text{ x } 157 = 423900W \quad (43)$$

The mean value of the efficiency turned out to be 99.91%.

5 DISCUSSION AND CONCLUSIONS

A discussion of the results and the conclusions drawn during the Master of Science thesis are presented in this chapter.

5.1 Discussion

The result of the simple lubrication model that was constructed without the use of the Helical 3D program showed higher values of the film thickness, of the order of 2 to 3 microns for almost all lubricants. This was an inaccurate model as the variations in contact loads (load sharing between the teeth) and velocities were not taken into consideration. However, the important inferences drawn from this model were that the film thickness is influenced highly by the speed and not so much by the load. Also, (Höglund, 1999) states that rapeseed oil is a good choice as a gear lubricant since it has the capacity to form a thicker film as well as having low fluid friction.

Next, with the introduction of the helical 3D program, load sharing and changes in the velocities showed realistic values of the film thickness, of the order of 1 micron, agreeing well with values stated in literature (Seireg, 1998). In the case of both spur and helical gears, a sudden drop in the film thickness was observed in the tip relief region, and from experimental tests performed at Scania, it was exactly in this region that a “pitting line” was formed.

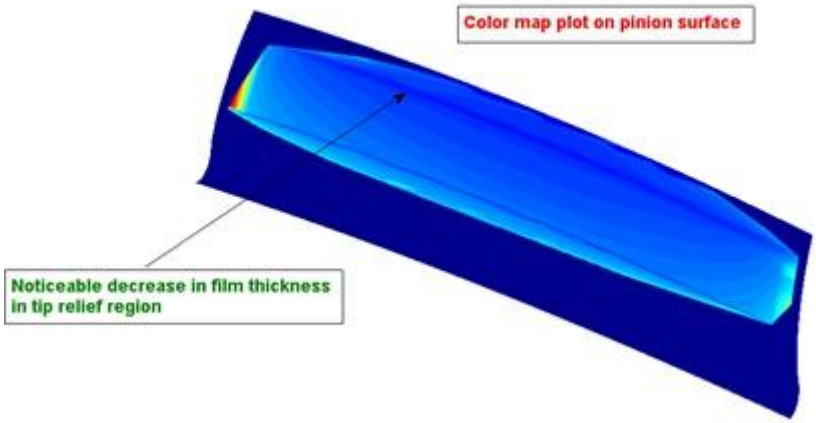

Figure 42, Film thickness plot on helical gear with modifications

Figure 43, Photograph showing “pitting” line in tip relief area on same helical gear (Courtesy Scania)

The two Figs. (42) and (43) can be considered a qualitative validation of this thesis since data of film thickness values determined earlier for the specific gear set was not available to make a proper validation. From the photograph, it can be observed that pitting has occurred in the area of the “mating gear tip relief”, i.e. the region where the tip relief of the mating gear comes into contact with the root of the pinion. The drop in film thickness can be seen along the same area, as shown in Fig. (42). However, no pitting is seen on the tip relief area of the pinion Fig. (43).

The thermal effects brought about a significant reduction in film thickness, about 25% in the case of spur gears and almost double that in the case of helical gears. The reduction was however proportional, they did not affect the manner in which the film thickness was distributed along the profile and face of the gear tooth.

A similar validation was made for the flash temperatures. In the regions where the flash temperatures are high, scuffing takes place.

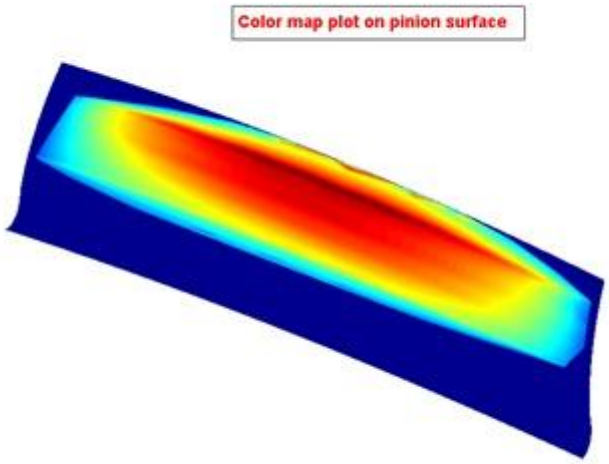

Figure 44, Plot of flash temperatures on helical gear surface

Figure 45, Scuffing marks seen on surface of middle tooth close to the tip (Courtesy Scania)

From the Fig. (44), it can be observed that high flash temperatures are present close to the tip. In the same area scuffing marks can be observed in the photograph shown in Fig. (45).

For the spur gear case, two types of tip relief modifications were investigated: linear and quadratic. It was concluded that a quadratic tip modification would be more suitable to avoid pitting in the tip relief area.
In order to investigate the reasons for the drop in film thickness, other parameters were also plotted; the relative radius of curvature was found to the main contributing factor.
The average value of 0.06 for the friction co-efficient was deemed quite reasonable (Scania).
Overall, the coupling of a lubrication model with a powerful gear contact analysis program is what makes this master thesis unique.

5.2 Conclusions

The following inferences were drawn and can be summarized as:

- A realistic lubrication model that takes into account profile modifications on gear teeth and thermal effects as a result of shear heating of the lubricant could be developed.
- The model predicts that the film thickness decreases in the tip relief region of the gear tooth and is indicative of an increase in the scope for pitting and wear. This effect can be avoided with the application of a quadratic tip relief having a suitable corner radius, as observed from the model.
- Further, the model also shows how thermal effects can reduce the film thickness significantly, more so in the case of helical gears than compared to spur gears.
- High values of the flash temperatures are observed in areas close to the tip and thereby increase the chances of scuffing in these regions.

6 RECOMMENDATIONS AND FUTURE WORK

In this chapter, recommendations on more detailed solutions and future work in this field are presented.

6.1 Recommendations

Understanding gear lubrication is tricky, as it entails a huge number of variables and the theory itself analogizes the gears in contact to two cylinders touching each other with a lubricating film in between. Achieving the perfect gear lubrication model can prove to be highly complex, as a number of effects such as starvation effects, transient thermal effects, side leakage, and non-newtonian behavior of the lubricant need to be taken into account (Wang et al, 2004). The inclusion of surface roughness only adds to this list of complexities. If an attempt were made to include the aforementioned, then a highly sophisticated gear lubrication model would have been developed.

In general, it is very hard to determine the dynamic loads (Larsson, 1997), this was however simplified with the use of the Helical 3D program. The variation in curvatures and velocities in the tip relief area could also be determined with Helical 3D, which was another added advantage. The inclusion of this program in the construction of the lubrication model proved to be very useful owing to its powerful contact analysis algorithm.

Values of the gear parameters obtained from the program at the extreme ends (root and tip, either extremes of the face) cannot be entirely trusted, owing to computational issues. However, if a proper interpolation of the remaining data can be made, this problem can somewhat be tackled.

6.2 Future work

The suggested extensions to the elastohydrodynamic lubrication model described in this thesis could be:

- Perform a detailed parameter analysis in order to check the influence of a number of variables on the film thickness, such as gears of different sizes, materials, different tip relief parameters, and lubricants other than mineral oil.
- Perform more detailed losses calculations, and validate with experimental observations.
- Implement a surface roughness model.
- Conduct analysis by refining the contact grid in Helical 3D; also perform a convergence test in order to avoid a too fine grid.
- A GUI (graphical user interface) that would enchance the utility to users. This could be in the form of an interactive screen enabling users to input data for different gears and lubricants and obtain plots of the film thickness instantly.
- Extend to other types of gears such as bevel, hypoid, and planetary as these are also made use of in transmissions and axles and an understanding of their lubrication is also necessary.

7 REFERENCES

Almqvist, Andreas. *Rough Surface Elastohydrodynamic Lubrication and Contact Mechanics*. Licentiate Thesis. Lulea University of Technology, 2004. Print.

Caika, V., Bukovnik, S., Offner, G., and Bartz, W.J. "*Elasto-hydrodynamic journal bearing model with pressure, temperature, and shear rate dependent viscosity*". Proc. International Conference on Tribology, Parma, Italy, 2006. Print.

Cameron, A. (1952) Hydrodynamic Theory in gear lubrication, *J. Inst. Petroleum*, Vol. 38, pp614-620.

Cheng, H.S. (1983) Elastohydrodynamic Lubrication, *CRC Handbook of Lubrication.,* Vol. II, pp139-148.

Cheng, H.S., and Wang, K.L. "*Thermal elasto-hydrodynamic Lubrication of spur gears*". NASA Contractor Report 3241, 1980.

Dowson, D., and Higginson, G.R. (1959) A numerical Solution to the elastohydrodynamic problem, *J. Mech. Engg. Science*, Vol. 1, pp6-15.

Dowson, D. and Higginson, G.R. *Elasto-hydrodynamic lubrication*: *The Fundamentals of Gear and Roller lubrication*. Oxford: Pergamon Press, 1966. Print.

Dudley, Darle W. *Handbook of Practical Gear Design*. 1st ed. New York: McGraw-Hill, 1984. Print.

Gohar, Ramsey. *Elastohydrodynamics*. 2nd ed. London: Imperial College Press, 2001. Print.

Gopinath, K., and Mayuram, M.M. *Module 2 –Gears*. Machine Design II, Online Lecture Notes, Indian Institute of Technology, Madras.

Gould, S.H. *Mathematics: Its Contents, Methods, and Meaning*. New York: Dover Publications, 1999. Print.

Hai, Xu. *Development of a generalized mechanical efficiency prediction methodology for gear pairs*. Thesis. Ohio State University, 2005. Print.

Hamrock, B.J. *Fundamentals of Fluid Film Lubrication*. NASA Reference Publication 1255, August, 1991. Print.

Helical 3D. Computer software. Web. <h*ttp://ansol.us/Products/Helical3D>/.*

H**ö**glund, Erik. (1999) Influence of lubricant properties on elastohydrodynamic lubrication, *J. Wear,* Vol. 232, pp176-184.

Larsson, Roland. (1997) Transient non-newtonian elasto-hydrodynamic analysis of an involute spur gear, *J. Wear*, Vol. 207, pp67-73.

Litvin, F. L., and A. Fuentes. *Gear Geometry and Applied Theory.* 2nd ed. Cambridge: Cambridge UP, 2004. Print.

Mordukhovich, G., and Anderson, N. (2002) Lubrication in Helical Gears, *Tribotest Journal*, Vol. 9, pp57-68.

Nijenbanning, G., Venner, C.H., and Moes, H. (1994) Film thickness in elastohydrodynamically lubricated elliptic contacts, *J. Wear*, Vol. 176, pp217-229.

Prakash, B., and Johansson, J. *1st report on gear transmission tribology project*. Technical Report. Lulea University of Technology, 2010. Print.

Rebbechi, B., and Townsend, D.P. "*Measurement of Gear tooth Dynamic friction*". Proc. From 7th International Power Transmission and Gearing Conference, San Diego, California, United States, 1996. Print.

Seireg, Shirley. *Friction and Lubrication in Mechanical design*. Taylor and Francis, 1998. Print.

Tobe, S. and Stolarski, T.A. *Rolling Contacts*. London: Professional Engineering publishing, 2000. Print.

Uicker, J.J., Pennock, G.R., Shigley, J.E. *Theory of machines and mechanisms*. USA: Oxford University Press, 2003. Print.

Van Beek, Anton. *Advanced Engineering Design: Lifetime performance and Reliability*. Delft: TU Delft, 2006. Print.

Wang, Y., Li, H., Tong, J., Yang, P. (2004) Transient thermoelastohydrodynamic analysis of an involute spur gear, *Tribology International*, Vol. 37, pp773-782.

APPENDIX A: GEAR DATA

This appendix contains the details of the two different gear sets used in this thesis: Standardized FZG Spur Gears and Standard Scania Helical Gears.

Table 5, Spur Gear data

Input Gear	Pinion
Input Torque	350 Nm
Input Speed	1500 r.p.m.
Center to center distance	91.5 mm
Number of teeth (Pinion)	16
Number of teeth (Gear)	24
Module	4.5 mm
Pressure angle	20
Pinion pitch diameter	73.2 mm

Table 6, Helical Gear data

Input gear	**Pinion**
Input Torque	2700 Nm
Input Speed	1500 r.p.m.
Center to center distance	160 mm
Number of teeth (Pinion)	20
Number of teeth (Gear)	46
Module	4.5 mm
Pressure Angle	20
Helix Angle	17
Pinion pitch diameter	96.96 mm

APPENDIX B: TOOTH FACE MATERIAL DATA

This appendix contains data pertaining to the gear material; note that the values are the same for both the spur and helical gears used in this thesis.

Table 7, Gear material data

Steel Grade	**17NiCrMoS6-4**
Young's Modulus of elasticity	2.06e11 N/m^2
Poisson's ratio	0.3
Thermal Conductivity	45 W/mK
Density	7800 Kg $/m^3$
Specific Heat	440 J/KgK

APPENDIX C: LUBRICANT DATA

Table 8, Data of the lubricant used

Lubricant	**Mineral oil**
Inlet temperature	$40^{o}C$
Viscosity	0.075 Pa-s
Pressure-viscosity coefficient	2.65e-8 Pa^{-1}
Thermal Conductivity	0.04 W/mK
Viscosity-temperature slope	0.0017 Pa-s/^{o}K

APPENDIX D: MISCELLANEOUS PLOTS

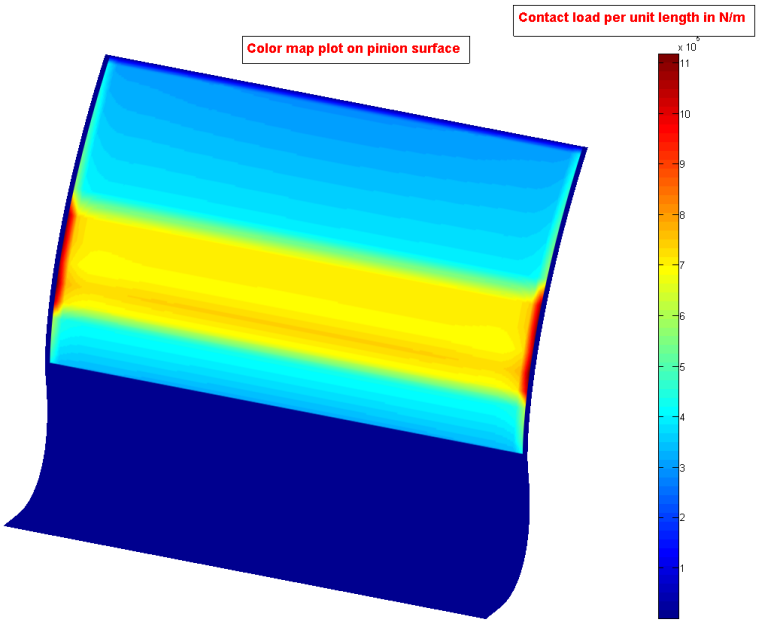

Figure 46, Plot of contact load per unit length for ordinary spur gear model

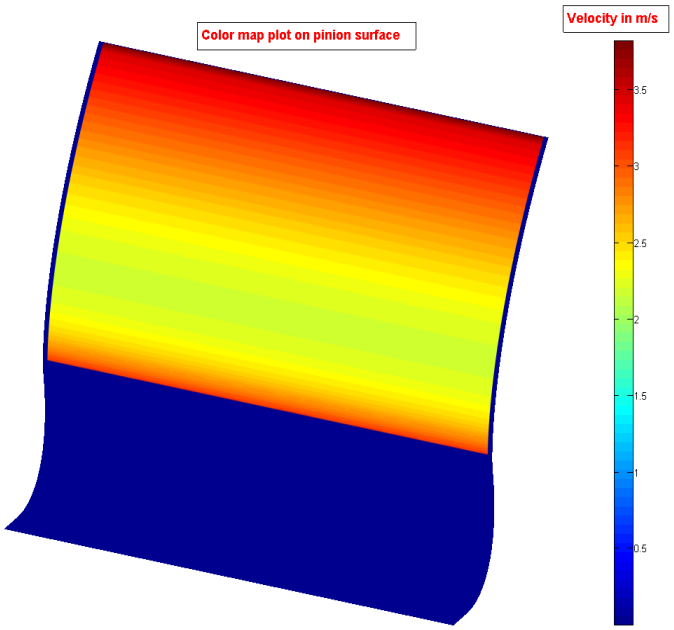

Figure 47, Plot of velocities for ordinary spur gear model

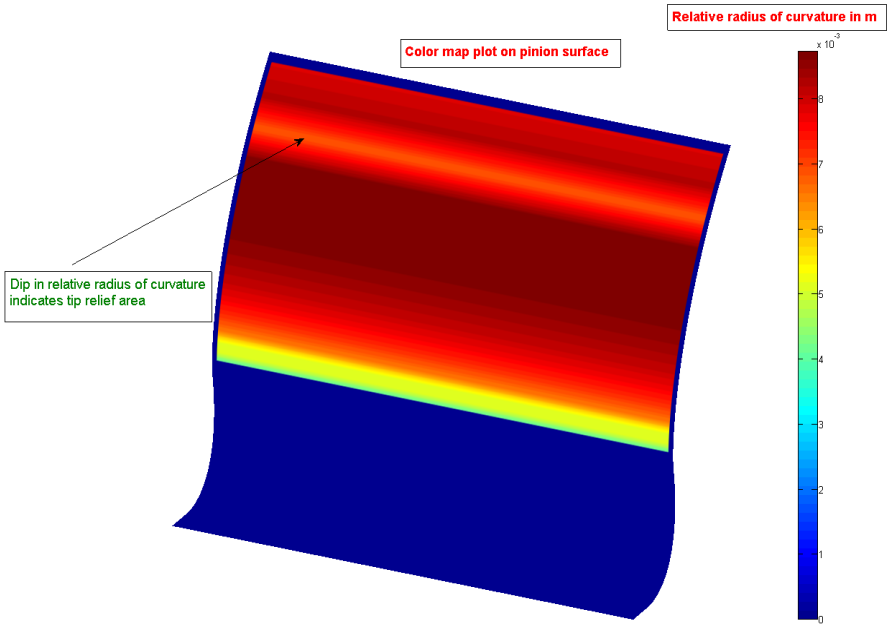

Figure 48, Plot of relative radius of curvature for spur gear model with linear tip relief

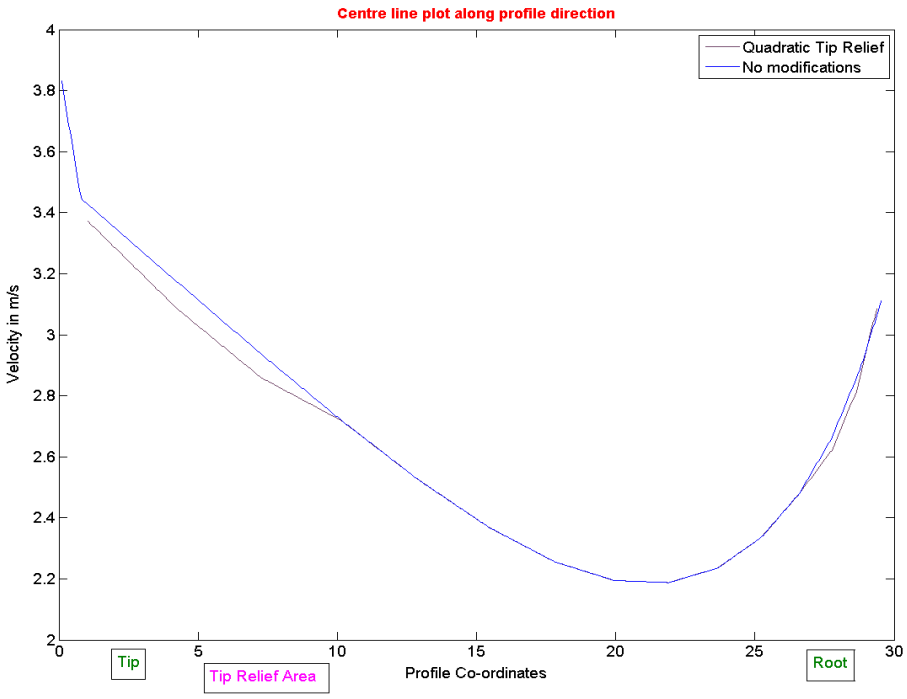

Figure 49, Centre line plot of velocity for spur gear model with quadratic tip relief

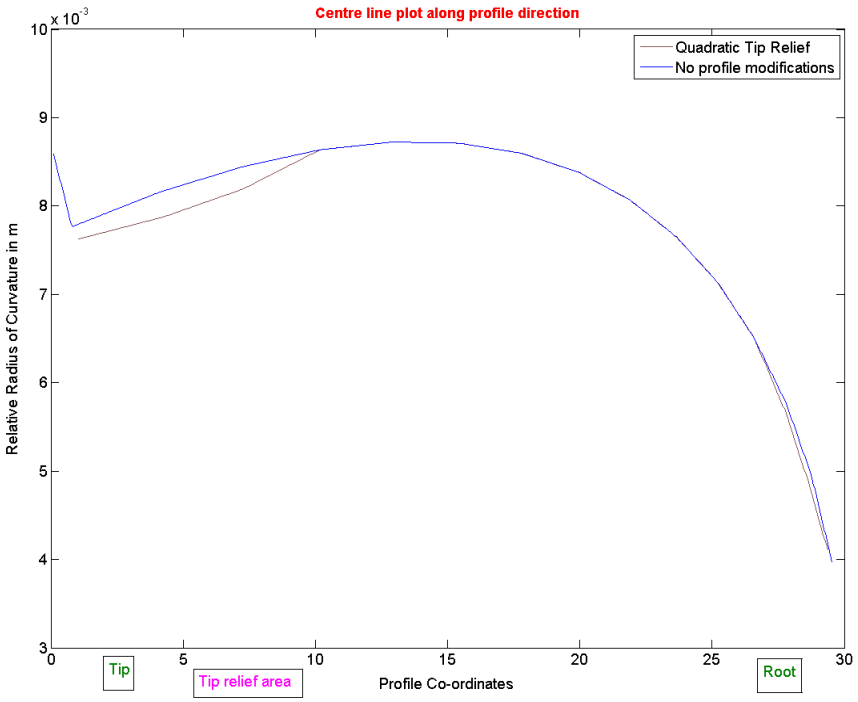

Figure 50, Centre line plot of radius of curvature for spur gear model with quadratic tip relief

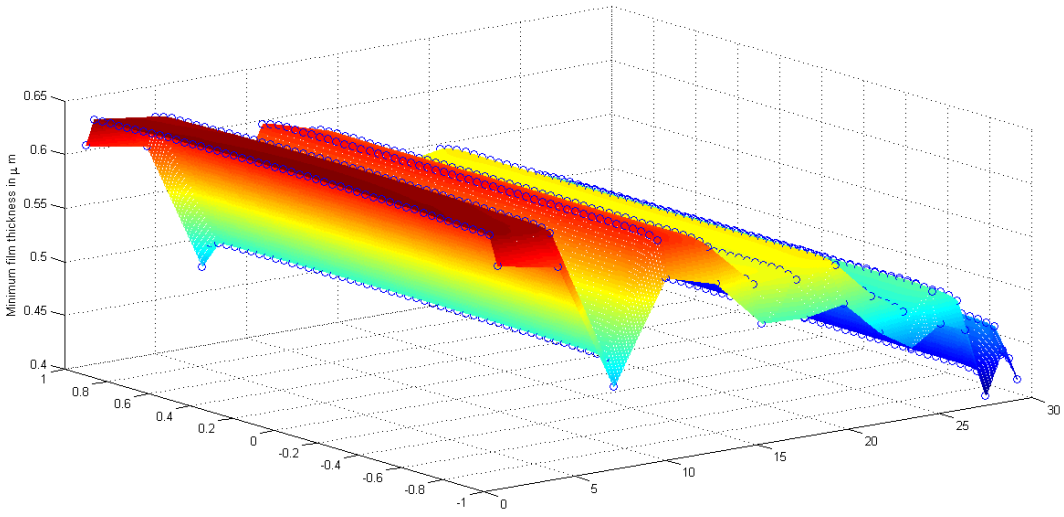

Figure 51, Surface plot illustrating variations across the face for the spur gear model with profile modifications and thermal effects

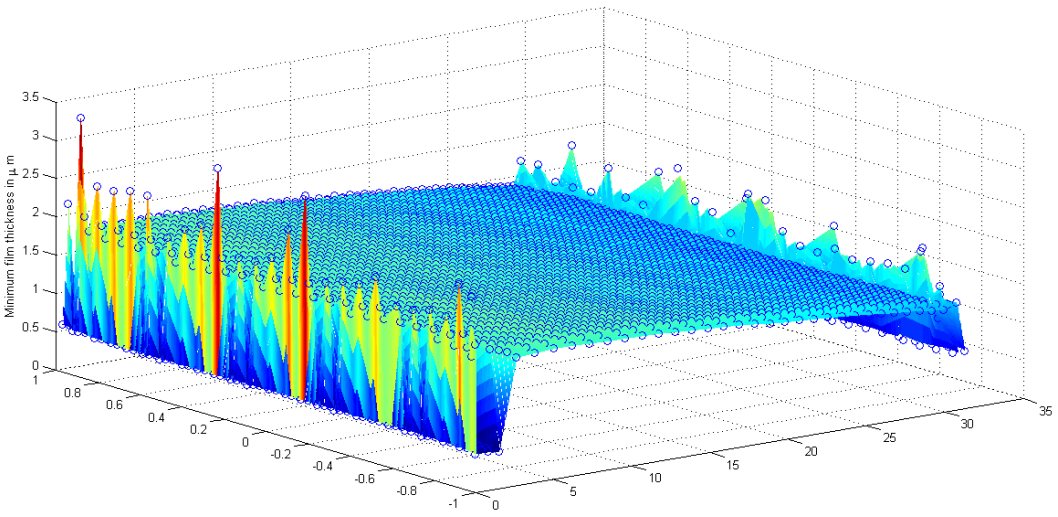

Figure 52, Surface plot illustrating variations along face for the ordinary helical gear model

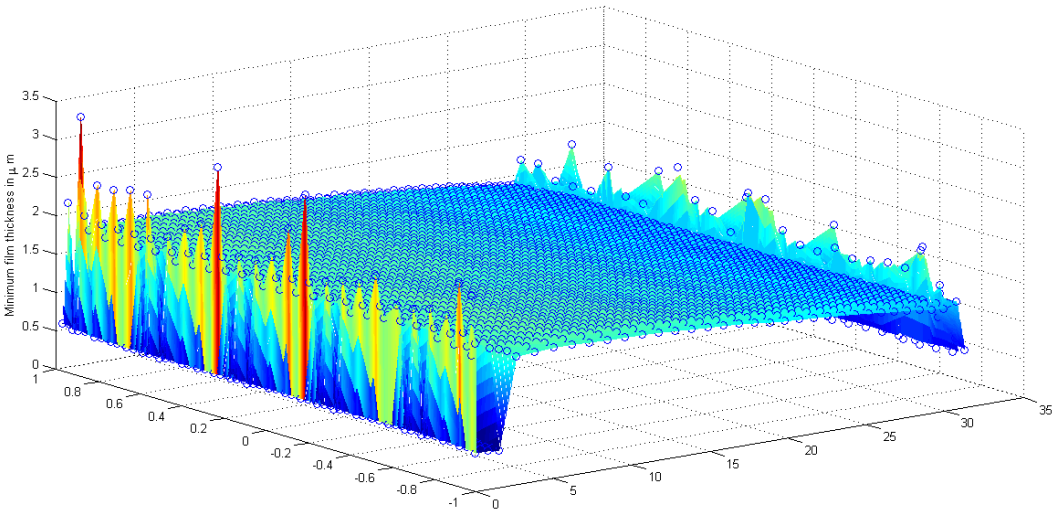

Figure 53, Surface plot illustrating variations along face for the helical gear model with modifications

APPENDIX E: ROUGHNESS PARAMETER TABLES

Table 9, Lubrication regimes for different spur gear models (method of finish: milling)

Type of lubricant model	**Lubrication regime**
Ordinary spur-no thermal effects	Boundary
Ordinary spur-thermal effects	Boundary
Spur with linear tip relief (no thermal effects)	Boundary
Spur with linear tip relief and thermal effects	Boundary
Spur with quadratic tip relief (no thermal effects)	Boundary
Spur with quadratic tip relief and thermal effects	Boundary

Table 10, Lubrication regimes for different spur gear models (method of finish: Hobbing and shaping)

Type of lubricant model	**Lubrication regime**
Ordinary spur-no thermal effects	Boundary
Ordinary spur-thermal effects	Boundary
Spur with linear tip relief (no thermal effects)	Boundary
Spur with linear tip relief and thermal effects	Boundary
Spur with quadratic tip relief (no thermal effects)	Boundary
Spur with quadratic tip relief and thermal effects	Boundary

Table 11, Lubrication regimes for different spur gear models (method of finish: Shaping and grinding)

Type of lubricant model	**Lubrication regime**
Ordinary spur-no thermal effects	Boundary
Ordinary spur-thermal effects	Boundary
Spur with linear tip relief (no thermal effects)	Boundary
Spur with linear tip relief and thermal effects	Boundary
Spur with quadratic tip relief (no thermal effects)	Boundary

Spur with quadratic tip relief and thermal effects	Boundary

Table 12, Lubrication regimes for different spur gear models (method of finish: Lapping)

Type of lubricant model	**Lubrication regime**
Ordinary spur-no thermal effects	Mixed
Ordinary spur-thermal effects	Boundary
Spur with linear tip relief (no thermal effects)	Mixed
Spur with linear tip relief and thermal effects	Boundary
Spur with quadratic tip relief (no thermal effects)	Mixed
Spur with quadratic tip relief and thermal effects	Boundary